



University of Kentucky  
UKnowledge

---

Theses and Dissertations--Mechanical  
Engineering

Mechanical Engineering

---

2018

## **$NO_x$ FORMATION IN LIGHT-HYDROCARBON, PREMIXED FLAMES**

Robert T. Hughes

University of Kentucky, rthughes94@gmail.com

Digital Object Identifier: <https://doi.org/10.13023/etd.2018.287>

[Right click to open a feedback form in a new tab to let us know how this document benefits you.](#)

---

### **Recommended Citation**

Hughes, Robert T., " $NO_x$  FORMATION IN LIGHT-HYDROCARBON, PREMIXED FLAMES" (2018). *Theses and Dissertations--Mechanical Engineering*. 118.

[https://uknowledge.uky.edu/me\\_etds/118](https://uknowledge.uky.edu/me_etds/118)

This Master's Thesis is brought to you for free and open access by the Mechanical Engineering at UKnowledge. It has been accepted for inclusion in Theses and Dissertations--Mechanical Engineering by an authorized administrator of UKnowledge. For more information, please contact [UKnowledge@lsv.uky.edu](mailto:UKnowledge@lsv.uky.edu).

## **STUDENT AGREEMENT:**

I represent that my thesis or dissertation and abstract are my original work. Proper attribution has been given to all outside sources. I understand that I am solely responsible for obtaining any needed copyright permissions. I have obtained needed written permission statement(s) from the owner(s) of each third-party copyrighted matter to be included in my work, allowing electronic distribution (if such use is not permitted by the fair use doctrine) which will be submitted to UKnowledge as Additional File.

I hereby grant to The University of Kentucky and its agents the irrevocable, non-exclusive, and royalty-free license to archive and make accessible my work in whole or in part in all forms of media, now or hereafter known. I agree that the document mentioned above may be made available immediately for worldwide access unless an embargo applies.

I retain all other ownership rights to the copyright of my work. I also retain the right to use in future works (such as articles or books) all or part of my work. I understand that I am free to register the copyright to my work.

## **REVIEW, APPROVAL AND ACCEPTANCE**

The document mentioned above has been reviewed and accepted by the student's advisor, on behalf of the advisory committee, and by the Director of Graduate Studies (DGS), on behalf of the program; we verify that this is the final, approved version of the student's thesis including all changes required by the advisory committee. The undersigned agree to abide by the statements above.

Robert T. Hughes, Student

Dr. Jose Graña-Otero, Major Professor

Dr. Haluk Karaca, Director of Graduate Studies

**$NO_x$  FORMATION IN LIGHT-HYDROCARBON, PREMIXED  
FLAMES**

---

THESIS

---

A thesis submitted in partial fulfillment of the requirements for the degree of  
Master of Science in Mechanical Engineering in the College of Engineering at the  
University of Kentucky

By

Robert Tyler Hughes

Lexington, Kentucky

Director: Dr. Jose Graña-Otero, Ph.D, Professor of Mechanical Engineering

Lexington, Kentucky

2018

Copyright © Robert Tyler Hughes 2018

## ABSTRACT OF THESIS

### $NO_x$ FORMATION IN LIGHT-HYDROCARBON, PREMIXED FLAMES

This study explores the reactions and related species of  $NO_x$  pollutants in methane flames in order to understand their production and consumption during the combustion process. To do this, several analytical simulations were run to explore the behavior of nitrogen species in the pre-flame, post-flame, and reaction layer regions. The results were then analyzed in order to identify all "steady-state" species in the flame as well as the determine all the unnecessary reactions and species that are not required to meet a defined accuracy. The reductions were then applied and proven to be viable.

KEYWORDS: Combustion,  $NO_x$ , Mechanism Reduction, Chemical Kinetics, Steady State Approximation

Robert Tyler Hughes

---

---

Date

$NO_x$  FORMATION IN LIGHT-HYDROCARBON, PREMIXED FLAMES

By

Robert Tyler Hughes

Dr. Jose Graña-Otero, Ph.D

---

Director of Thesis

Dr. Haluk Karaca, Ph.D

---

Director of Graduate Studies

# Acknowledgements

The following thesis, while an individual work, benefited greatly from the guidance and time of several people. First, my advisor, Dr. Jose Graña-Otero, spent countless hours guiding me and shaping my graduate level knowledge. I would also like to thank my committee of Dr. Michael Renfro, Dr. Alexander Martin, and Dr. Bradley Berron. Each one challenged my thinking and asked insightful questions that guided me to present my research in the best way possible. Finally, I would like to also thank Siamak Mahmoudi and Simon Schmitt from my lab as they both assisted me with technical knowledge and thoughts on the results I was obtaining.

# Contents

Acknowledgements	iii
List of Figures	v
List of Tables	viii
<b>1 Introduction</b>	<b>1</b>
<b>2 Literature Review</b>	<b>3</b>
2.1 A Brief History of Chemical Kinetics . . . . .	3
2.2 <i>NO</i> Pathways . . . . .	4
2.3 Previous Reduction Methods . . . . .	7
2.4 Uniqueness of Mechanism Reduction . . . . .	8
<b>3 Methods</b>	<b>10</b>
3.1 Introduction . . . . .	10
3.2 Mechanism Comparison . . . . .	14
3.3 Mechanism Analysis . . . . .	17
3.4 Steady State . . . . .	22
<b>4 Results</b>	<b>25</b>
4.1 <i>NO</i> Analysis . . . . .	25
4.2 <i>NO</i> <sub>2</sub> Analysis . . . . .	35
4.3 Overview . . . . .	43
<b>5 Conclusion</b>	<b>49</b>
<b>Appendix</b>	<b>50</b>
<b>References</b>	<b>64</b>
<b>Vita</b>	<b>66</b>

# List of Figures

1	Flame Regions . . . . .	12
2	More Prominent Nitrogen Based Species Concentrations . . . . .	13
3	Less Prominent Nitrogen Based Species Concentrations . . . . .	14
4	Comparison of GRI-Mech 3.0, Lu, and Lu + SD . . . . .	15
5	Comparison of Radicals Between GRI-Mech 3.0 and Lu + SD Mech- anisms . . . . .	16
6	Comparison of Nitrogen Based Species Between GRI-Mech 3.0 and Lu + SD . . . . .	17
7	NO Consumption Reactions . . . . .	19
8	NO Production Reactions . . . . .	20
9	NO Consumption Surface Plot . . . . .	21
10	NO Production Surface Plot . . . . .	21
11	NO Consumption Contour Plot . . . . .	21
12	NO Production Contour Plot . . . . .	21
13	CN Steady State Approximation . . . . .	23
14	HCN Steady State Approximation . . . . .	23
15	NO Production Surface Plot . . . . .	25
16	NO Production Contour Plot . . . . .	25
17	NO Production Reaction Layer Contour Plot . . . . .	26
18	NO Production Post Flame Contour Plot . . . . .	26
19	NO Consumption Surface Plot . . . . .	26
20	NO Consumption Contour Plot . . . . .	26
21	NO Consumption Reaction Layer Contour Plot . . . . .	27
22	NO Consumption Post Flame Contour Plot . . . . .	27
23	NO Consumption Reactions . . . . .	29
24	NO Consumption Reactions Enlarged . . . . .	30
25	NO Consumption Reactions . . . . .	30
26	NO Reaction Layer Production Reactions . . . . .	33
27	NO Post Flame Production Reactions . . . . .	33
28	NO Steady State Approximation . . . . .	35
29	NO <sub>2</sub> Production Surface Plot . . . . .	36
30	NO <sub>2</sub> Production Contour Plot . . . . .	36
31	NO <sub>2</sub> Production Reaction Layer Contour Plot . . . . .	36
32	NO <sub>2</sub> Production Post Flame Contour Plot . . . . .	36
33	NO <sub>2</sub> Consumption Surface Plot . . . . .	37
34	NO <sub>2</sub> Consumption Contour Plot . . . . .	37
35	NO <sub>2</sub> Consumption Reaction Layer Contour Plot . . . . .	37
36	NO <sub>2</sub> Consumption Post Flame Contour Plot . . . . .	37
37	NO <sub>2</sub> Reaction Layer Consumption Reactions . . . . .	38
38	NO <sub>2</sub> Post Flame Consumption Reactions . . . . .	39
39	NO <sub>2</sub> Reaction Layer Production Reactions . . . . .	40
40	NO <sub>2</sub> Post Flame Production Reactions . . . . .	41
41	NO <sub>2</sub> Steady State Approximation . . . . .	42
42	NO Mechanism Reduction Test . . . . .	47
43	NO <sub>2</sub> Mechanism Reduction Test . . . . .	48

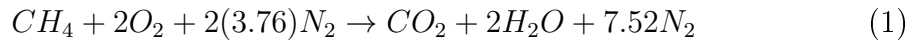


## List of Tables

1	<i>CN</i> Consumption Reactions . . . . .	23
2	<i>CN</i> Production Reactions . . . . .	23
3	<i>NO</i> Consumption Pre-Heat Region . . . . .	27
4	<i>NO</i> Consumption Reaction Layer . . . . .	28
5	<i>NO</i> Consumption Post Flame . . . . .	28
6	<i>NO</i> Production Pre-Heat Region . . . . .	31
7	<i>NO</i> Production Reaction Layer . . . . .	31
8	<i>NO</i> Production Post Flame . . . . .	32
9	<i>NO</i> Required Reactions . . . . .	34
10	<i>NO</i> Required Reactions Continued . . . . .	34
11	<i>NO</i> <sub>2</sub> Consumption Pre-Heat Region . . . . .	37
12	<i>NO</i> <sub>2</sub> Consumption Reaction Layer . . . . .	38
13	<i>NO</i> <sub>2</sub> Consumption Post Flame Region . . . . .	38
14	<i>NO</i> <sub>2</sub> Consumption Pre-Heat Region . . . . .	39
15	<i>NO</i> <sub>2</sub> Production Reaction Layer . . . . .	39
16	<i>NO</i> <sub>2</sub> Production Post Flame . . . . .	40
17	<i>NO</i> <sub>2</sub> Required Reactions . . . . .	41
18	Steady State Species Approximation . . . . .	43

# 1 Introduction

In today's day in age, being as environmentally friendly as possible has become one of the most important qualities in the technological industry. Combustion is used in some form in just about every industry and has a negative environmental impact. The combustion phenomena is the main process used to harness energy from fuels. One of the problems with combustion is that it is not very efficient and produces a family of highly reactive and poisonous gas called  $NO_x$ . These nitrogen oxides react with volatile organic compounds in sunlight and can create both ozone,  $O_3$ , and PM, particulate matter. Ozone in the upper atmosphere can be beneficial by reflecting UV rays, but high concentrations of around 100 ppb can be harmful to the respiratory system of plants, animals, and humans [1]. Particulate matter is damaging to the respiratory system as well because the tiny particles can be inhaled and can find their way into the bloodstream. In order to limit the output of PM and  $O_3$ , the formation of  $NO_x$  must be studied. In order to understand  $NO_x$  at its core, it is best to begin with the simplest flame case possible. This simple case allows for a basis to be established before more complex flame cases can be assessed. First, basic combustion is described as the reaction between a fuel and an oxidizer and the main chemical reaction used in this study can be shown in equation 1 where the fuel is methane,  $CH_4$ , and air as the oxidizer. Since methane is made up of only one carbon and four hydrogen molecules, it is the lightest, most simple, carbon based fuel that can be used for simulation.



Although this equation seems relatively trivial, it does not visually represent the hundreds of intermediate reactions that occur between the reactants and products. These intermediate reaction are responsible for the creation of lower concentration species in the flame. Among these lower concentration species is where  $NO_x$  species can be found. Even though these pollutants have several order of magnitudes of concentration less than more prominent species, such as  $H_2O$  and  $CO_2$ , they still have adverse affects on the environment in low quantities. The reason  $NO_x$  is such a burden to manipulate is because they require large amounts of energy for them to react with other species. In a typical combustion process  $NO_x$  would not be an issue if the temperature of the flame slowly decreased from the flame temperature down to the ambient temperature. In this case,  $NO$  and  $NO_2$  would initially be formed and then, after a significant amount of time, eventually dissociate back into molecular nitrogen. Since this slow decrease in temperature is not practical,  $NO$  and  $NO_2$  are formed in the high temperatures of the flame and progress quickly through the reaction layer. Then, before  $NO_x$  can be converted back to molecular nitrogen, the flow mixes with ambient air. The ambient air rapidly cools or "quenches" the nitrous oxides, thus eliminating the possibility of them reacting with any other species at a significant rate. Thus, the only way to cause  $NO_x$  to react with other species is to add a catalyst. Catalysts are used to lower the amount of required energy for the  $NO_x$  species to react with other species without heat addition. The use of this catalyst is already the main solution to  $NO_x$  production in most vehicles. Although the catalytic converter does reduce the output of nitrous oxides, the

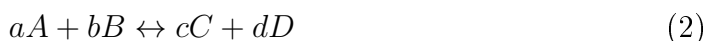
species used are very expensive and are not practical for all applications. The main goal of this project is to understand the chemical kinetics behind the formation of these  $NO_x$  pollutants. Through this understanding, the reactions responsible for the creation of  $NO_x$  may be able to be influenced to limit the generation of these pollutants. The process used to analyze the chemical kinetics of  $NO_x$  can also be used to simplify numerical flame simulations. This process can identify and remove any unnecessary reactions contained in a reaction mechanism by comparing their reaction rate magnitudes. Then, the reactions that do not have a significant influence on the production or consumption of  $NO_x$  can be removed. One application of the mechanism reduction is to simplify flame simulation calculations. In turbulent flows, the five conservation equations have to be calculated at each node: conservation of mass, conservation of energy, and the conservation of momentum in each Cartesian direction. Depending on how fine of a mesh is chosen, there could be thousands or even millions of nodes. Therefore, these calculations require large amounts of computing power and can take a significant amount of time to complete. Now, when considering turbulent flames, the calculations must still take the five conservation equations into account as well as an additional equation for every single species. These species then require several of their own reactions to calculate their production and consumption at each given node. On top of all these equations, the transport equation must be defined at each node for each species as well. For most modern computers, this task is not feasible in a reasonable amount of time. Hence, if the number of reactions required from the mechanism at each node in the mesh can be reduced, it will significantly reduce the time to perform the calculations. Again, the main goal of this study is to discover the reactions and species behind the production and consumption of  $NO_x$ . In order to achieve this goal, a  $NO_x$  mechanism must be reduced to highlight the main reactions and species that produce these pollutants with controlled accuracy. The process to do so will be discussed using properties of chemical kinetics from physical chemistry. The algorithm developed has been proven to reduce the  $NO_x$  mechanism between 20-30% while maintaining a reasonable associated error. The main benchmarks established for this project were 90%, 95%, and 99%. The 90% accuracy is considered acceptable because the constants in the mechanisms have been experimentally measured within a range of 10% error as well.

## 2 Literature Review

The main focus of this literature review is to discuss the history of chemical kinetics and how the main principles are applied. The principles behind chemical kinetics have been widely used in research to quantify chemical phenomena. This review will explore how these principles were used in the past and how this study takes a different approach.

### 2.1 A Brief History of Chemical Kinetics

As stated before, the main focus of this study is based around the formation of  $NO_x$ , therefore, a brief history of chemical kinetics will first be discussed. Chemical kinetics is defined as the study of reactions through their reaction rates that occur during a specific process. Chemical kinetics stemmed from the law of mass action discovered by Guldberg and Waage in Norway in 1864. They proposed that the rate of a given chemical reaction is proportional to the product of the molar mass of the reactants [3]. The law of mass action considers the reaction between two species and defines the relationship between the concentrations of the reactants and products to the equilibrium constant. If the reaction considered is



where  $a$ ,  $b$ ,  $c$ , and  $d$  are the molar coefficients and  $A$ ,  $B$ ,  $C$ , and  $D$  are the species of the reaction. Thus, the following relationship can be defined for equilibrium constant  $k$ .

$$k = \frac{[A]^a[B]^b}{[C]^c[D]^d} \quad (3)$$

One year later, August Harcourt and William Esson, a physicist and mathematician at Oxford, conducted studies of the reactions between Hydrogen Dioxide and Hydrogen Iodide. The result was a relationship between the concentration of a given species and time. Their experiments also suggested that there exists a temperature dependence for the reaction rate [4]. Surprisingly, in their research they did not use an assumption of absolute 0, but instead measured it experimentally and found a very close temperature of  $272.6^\circ C$  compared to the accepted value of  $273.15^\circ C$ . Their relationship proposed that the reaction rate was a function of a frequency factor,  $A$ , temperature,  $T$ , and a reaction constant,  $C$ .

$$k = AT^C \quad (4)$$

In 1884, a Dutch physical chemist, Jacobus van't Hoff, continued the work of Harcourt and Esson and published his book, *Studies of Chemical Dynamics*. In the text, van't Hoff proposed what is now called the 'van't Hoff equation', which relates reaction rate constant to the change in temperature for the given change of enthalpy [5]. This equation has been widely used in the advancement of chemical and thermodynamic research. The equation is defined as

$$\ln(K_c) = \frac{-\delta H^\circ}{R} \frac{1}{T} + \frac{\delta S^\circ}{R} \quad (5)$$

where  $K_c$  is the equilibrium constant,  $H$  is the enthalpy of formation,  $S$  is the entropy of formation,  $R$  is the universal gas constant, and  $T$  is the temperature in Kelvin. He claimed that  $K_C$  is the ratio of  $k_1$  and  $k_{-1}$  which are the rate constants of the forward and reverse directions of the reaction. van't Hoff was the first to claim that a reaction could be considered to be reversible.

Friedrich Wilhelm Ostwald, a German chemist and 1909 Nobel Prize in chemistry recipient, published his *Outlines of General Chemistry* in 1887 in which he introduced the ideas of half-life and reaction order [6]. Half life is described as the time it takes for an initial concentration to reduce to half the original amount. His method was that if the concentration of one species was held constant and the concentrations of the rest were taken in excess, then the change in concentration of the species taken in excess will depend on the rate of change of the species of original concentration. Conducting this process for each species will determine which species is the slowest and thus, the reaction order. Finally, Svante Arrhenius, a Swedish chemist, continued the work of van't Hoff and was known as one of the founders of physical chemistry. His work in physical chemistry earned him the Nobel prize for Chemistry in 1903. He was first to introduce the 'Arrhenius equation' which relates the reaction rate of a given reaction to the universal gas constant, temperature, and activation energy. Before Arrhenius, no one had considered the idea of a reaction having an activation energy which is the minimum amount of energy required for a chemical reaction to begin. He was able to use his discoveries to relate the temperature of the ground as a function of the concentration of Carbonic Acid in the air [7]. This revolutionary paper was the first research to prove that humans were having an adverse effect on the planet through the production of  $CO_2$ . the Arrhenius equation provides a way to calculate the rate reactions for all the reversible reactions in the combustion mechanism. The calculation of these reaction rates are crucial to the algorithm used in this study to find the reductions in the mechanism.

Now, the first person to suggest the idea of the steady state hypothesis was David Leonard Chapman, an English physical chemist at Oxford. In 1913, he published a paper that introduced the idea of a 'steady state' process [8]. Continuing the research of Chapman, Max Bodenstein, a German physical chemist, conducted research using the quasi-steady state approximation to determine the reaction's rate equation. The reason this approximation is valid is because Bodenstein proved that when an overall reaction is decomposed into its basic steps, the concentrations of the intermediate species will remain quasi-constant. Therefore, their variations can be neglected and thus, can relate the concentrations of the reactants to the reaction rates [9].

## 2.2 NO Pathways

Since this project was based around the  $NO_x$  mechanism in a flame, the history of  $NO$  pathways will be discussed. Currently, the theory for the production of  $NO$  is described in three pathways: thermal  $NO$ , prompt  $NO$ , and fuel-bound

*NO* mechanisms. First, the thermal pathway, originally introduced by B. Y. Zel'dovich, is widely known as the main source of the production of *NO*. Thermal *NO* is found in the high temperature regions of the flame, around  $T > 1700K$ . This pathway can be described as one main reaction



as well as three intermediate reactions



Now these reactions can be used to quantify the production rate of *NO* through the thermal pathway detailed in equation 10.

$$[NO] = k_5[O][N_2] + k_6[N][O_2] + k_7[OH][N] \quad (10)$$

where  $k_7$ ,  $k_8$ , and  $k_9$  are the reaction rates for equations 7, 8, and 9 respectively. The thermal pathway is generally very slow because the rate determining reaction, equation 7, is very slow due to its high activation energy and therefore requires a high temperature to increase the reaction rate [10].

Next, the prompt *NO* pathway was proposed by C. P. Fenimore in 1971 [11].

Prompt *NO* occurs in fuel-rich regions of the flame, around  $T \approx 1400K$ .

Therefore, prompt *NO* occurs before thermal *NO* because the flame has not reached high enough temperatures for thermal *NO* to be relevant. Fenimore's mechanism has several steps that occur before any *NO* is produce. He originally proposed the mechanism to consist of



then, later included the reactions



where these reactions mainly produce *HCN*. The reactions in the next step in the pathway generally produce molecular nitrogen where reactions 11, 13, and 14 produce *HCN*. The *HCN* molecules then react with molecular oxygen to form *NCO* and then *NCO* reacts with molecular hydrogen to form *NH*. Then *NH* reacts with either *H* or *OH* to produce the molecular *N*. This process can be seen from the following reactions.





Finally, the molecular nitrogen reacts with  $OH$  or  $O_2$  to produce  $NO$  through the reactions

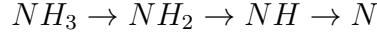


Therefore, prompt  $NO$  is the main source of  $NO$  production at the beginning of the flame until the temperature of the flame is high enough for thermal  $NO$  to be relevant.

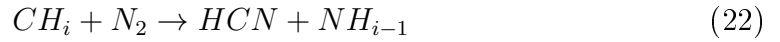
The last pathway for  $NO$  formation is the fuel-bound nitrogen pathway. This pathway occurs from the thermal decomposition of fuel-bound nitrogen that produce lower-weight nitrogen compounds ( $NH_3$ ,  $NH_2$ ,  $NH$ ,  $HCN$ ,  $CN$ ) [12]. The thermal decomposition of these fuel-bound species can be described through the general reaction



where  $NH_i$  eventually decomposes to molecular nitrogen



The intermediate reactions that lead to the formation of  $NO$  in this pathway are



which eventually form  $NO$  through  $NH$  and  $CN$  reacting with diatomic oxygen.





All of these pathways can be seen throughout the analysis of the intermediate reactions of  $NO_x$  species. The main reactions for each pathway can be identified and can be ranked on importance at different points in the flame. Obviously, in the higher temperature region of the flame, the thermal  $NO$  pathway will dominate, while at lower temperatures, the prompt  $NO$  pathway will generate the majority of  $NO$ .

## 2.3 Previous Reduction Methods

Mechanism reduction has become a popular area of research in the past few decades. All sorts of algorithms have been used to find ways to reduce the size of these mechanisms to reduce computing time for turbulent flame simulations. Dr. Michael Frenklach of the University of California Berkley, has published several papers on the subject of mechanism reduction. In the first few papers, Frenklach et al. propose that the best way to find the reactions that do not contribute a significant amount is by comparing them with a chosen reference reaction. They suggest that the reference reaction could be anything from the rate limiting step to the fastest reaction rate. Then they would remove any reaction that was found to be unnecessary and the error attributed to its removal was found [13-16]. Another method of mechanism reduction proposed by Frenklach et al. is solution mapping. Solution mapping defines a vector of all species as a function of state variables (concentrations, temperature, etc.) and compares the pathway for all the reactions to computing time [17]. This highlights the reactions and involved species that take up the majority of the computing power. These species and reactions can then be analyzed and determined if their removal is more beneficial than harmful. In other words, is the error created from removing the reactions or species worth the savings in computing power. These reduction can then be checked to see how they effect the chosen independent flame responses: ignition delay times, radical concentrations, and laminar flame speed. As some have done in the past, Lu et al. have developed a process for reducing a mechanism through a process of 'skeletal reduction' in which they eliminate then unimportant species and reactions based on the application of the mechanism. Previously, the two main reduction processes were through rate analysis and Jacobian analysis [18-20]. The rate analysis assumes that a species can be eliminated if it does not create significant error in the other species. The Jacobian method determines the importance of lesser species through their coupling with more important species. Along with the skeletal reduction, Lu et al. also considered the applications of partial equilibrium and the quasi-steady state (QSS) assumption. In their study, they generated their skeletal mechanism through the theory of direct relation graph (DRG) to identify the unimportant species along with their unnecessary reactions. The DRG essentially couples all species that depend on each other and determines the error involved in removing that species. If the removed species is involved in several couplings, its removal can cause a great amount of error. After developing the skeletal mechanisms, Lu et al. reduced the mechanism even further through the QSS approximation. The QSS approximation was conducted to each species that met the criteria in order



to simplify the amount of numerical calculations that needed to be made. Continuing the work of Frenklach et al. and Lu et al., Pepiot-Desjardins et al. proposed several techniques for the large reaction mechanisms. First, they defined the chemical feature they were aiming to maintain, whether it be flame speed, ignition properties, ect. Then they defined the two methods they focused on as the direct relation graph method (DRG) and the computational singular perturbation theory (CSP). Again, the DRG method focuses on the production rate analysis while the CSP method relies on time scale analysis. In other words, the DRG method is based around relating each species to one another and evaluating the effects if one was to be removed. On the other hand, the CSP method compares the two species through their rate determining reaction. They were also able to apply the steady state approximation to determine which species did not require the calculation of their transport properties [21]. Several papers use the DRG method in reducing mechanisms for their research calculations including Xin et al. who used this process to model the process of oxidative coupling of methane [22].

## 2.4 Uniqueness of Mechanism Reduction

Although this study uses some of the same principles used for mechanism reduction in the past, there are still several qualities that allow it to stand on its own. First, the similarities include the process of the skeletal reduction through comparison of reaction rates. Also, the continued reduction of the mechanism uses the quasi-steady state assumptions to identify the steady state species. These are they two main similarities used from the existing literature. Now, the past studies have been focused on the entire mechanism with only the flame characteristics in mind, such as, flame speed. The algorithm used for this project uses rate asymptotics in the mechanism reduction process. The rate asymptotics compare the magnitudes of the reaction rates and determines the amount of reactions that need to be kept for each location in the flame. This process allows for the user to predetermine the desired accuracy when conducting the mechanism reduction. Another main difference is that the past studies remove the majority of the lower concentration species because their contribution to the different flame characteristics are negligible. Conversely, the procedures for this mechanism are focused around the lesser concentration species because that is where the nitrogen based species are produced. If the mechanism in question does not require  $NO_x$  chemistry then they can typically be removed with other lesser reactions, but when considering  $NO_x$ , the lesser reactions must be kept which is proven later on in the paper. The reduction procedure for this project also is split into the three regions of the flame which, previously, has not been done. If another researcher is only studying a certain portion of the flame, then this reduction process can focus the reduction around the region in question. Several of the previous literary works conduct their skeletal reductions without the knowledge of the resulting error that will come out of their process. The algorithm used for the skeletal reduction of the  $NO_x$  mechanism in this study have predetermined error benchmarks. Although the benchmarks were set at 90%, 95%, and 99% for this project, any chosen benchmark can easily be applied to the algorithm. This allows for researchers to determine how important their

accuracy is versus the resultant computing time. Finally, these reductions are based around the individual species themselves, there is no coupling analysis. If a nitrogen based species is present in the production of another nitrogen based species that has already been deemed necessary, then it is also kept and reduced to the preset benchmark accuracy. This allows for the potential formation of individual species mechanisms in which, say a reaction for species A, is important in the production of B, but not the reverse then that reaction would only be present in the mechanism for species B. Therefore, that reaction can be removed from the mechanism for A and cut down on computing time.

## 3 Methods

### 3.1 Introduction

In order to understand the formation of the intermediate species during the combustion process, the intermediate reaction rates can be analyzed throughout the simulated flame. To begin, the reaction constants can be calculated by using the Arrhenius equation developed by Svante Arrhenius. He developed the relation between reaction constants and temperature defined by

$$k = Ae^{\frac{-E_A}{RT}} \quad (30)$$

where  $k$  is the rate constant,  $A$  is the frequency factor,  $E_A$  is the activation energy,  $R$  is the gas constant, and  $T$  is the temperature in Kelvin.

Using these calculated reaction constants, the reactions rates can be evaluated at a certain point in the flame. The reaction rates are calculated by multiplying the reaction constant with the concentrations of the reactant. The magnitudes of these reaction rates are what are used in the reaction asymptotic analysis where the magnitude of the reaction rate expresses how fast a species is being produced or consumed. Analysis of these rates for  $NO_x$  species reactions can map out their behavior by ranking their magnitudes.

Now, as stated before,  $NO_x$  pollutants are formed at very high temperatures and do not dissipate after leaving the flame. The reason  $NO_x$  species do not decay is because they contain a very high activation energy. Since the Arrhenius equations has a negative exponent with the activation energy as the numerator and  $R$  is a constant, then the only way for  $NO_x$  to form in a significant amount is at very high temperatures. High temperatures in the flame are not a problem, however, as soon as the  $NO_x$  species leave the high temperatures, they become inert or "quenched". This is because the magnitude of the reaction constant will be much smaller in cooler temperatures, resulting in a much smaller, almost non-existent, reaction rate. Therefore, the magnitude of concentration the  $NO_x$  species leave the flame with is the concentration at which they will remain.

While it is relatively easy to model the formation of  $NO_x$  in laminar combustion, the majority of combustion processes used in energy production are turbulent flows. In order to analyze what happens inside the flame, computer simulations can be developed. The computer software used to simulate the flames for this research project was Cantera. Cantera is an open source software project that can calculate thermodynamic, chemical kinetic, and transport calculations. The Cantera software was started by Professor David G. Goodwin at the California Institute of Technology. [2] For Cantera to calculate flame simulations, the software must be given reactions mechanisms from the user. These mechanisms contain all species and reactions involved throughout the entirety of the flame and usually are developed from experimentation. Depending on the complexity of the flame, these mechanisms can have ten's of species and hundred's of intermediate reactions. Since most of the flames studied in  $NO_x$  formation are turbulent, the calculations are much more complex and require a lot more computing power. In some cases, simulations can take several days to conduct and some months. Although computing power is exponentially growing, there are still steps that can be taken to reduce the amount of calculations the

software has to process. Using the Arrhenius equation, the reactions for  $NO_x$  species can be analyzed and determined if they have a significance at every point in the flame.

The flame studied in this research project was a lean, planar, adiabatic, 1D, laminar flame. It was studied at an equivalence ratio of  $\phi = 0.8$ , where the equivalence ratio can be calculated using equation 3.

$$\phi = \frac{(\frac{A}{F})_{Stoich}}{\frac{A}{F}} \quad (31)$$

where  $A$  is the number of moles of air and  $F$  is the number of moles of fuel taken from equation 1. The numerator is the air to fuel ration when equation 1 is stoichiometric and the denominator is the air to fuel ratio of the flame. This value was chosen because the majority of combustion processes are run at lean conditions so no fuel goes unburnt.

Now, this study considers the three different sections of the flame: the pre-heat region, the reaction layer, and the post-flame region. The pre-heat region is where the mixture of fuel and air is beginning to increase in temperature, but has not yet begun to react at a significant rate. The reaction layer is where the majority of reactions begin to occur and the visible flame sheet appears. This region can be determined by locating the maximum concentration of  $CH$  as its center. The actual thickness of the reaction layer can vary depending on the ambient conditions. Therefore, the reaction layer in all of the plots begins where the fuel concentration of fuel begins to drop and ends where the final concentrations of  $H_2O$  and  $O_2$  plateau. Finally, the post-flame region is considered to be the region after the reaction layer where the flame sheet is not visible anymore. This region is where the  $NO_x$  species are quenched and do not react with any other species and they converge on their final concentration. These regions can be seen in figure 1 where the lightest region is the pre-heat region, the center region is the reaction layer, and the darkest is the post-flame region.

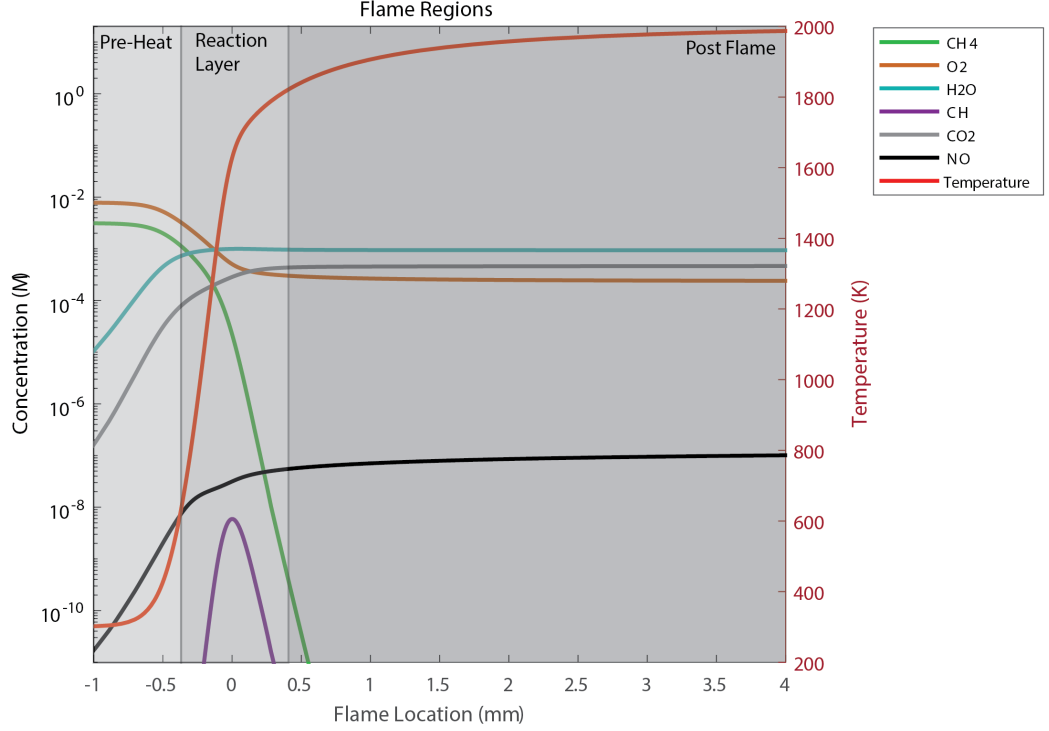


Figure 1: Flame Regions

Figure 1 illustrates the expected behavior of each region. It is plain to see that in the pre-heat region, the temperature is increasing through the beginning of our reaction layer. At the boundary of the pre-heat region and the reaction layer, the concentration of fuel,  $CH_4$ , begins to decline. This declination is because the fuel is being consumed and it converges to approximately zero by the end of the reaction layer. Since this flame was defined as a lean flame, the concentration of  $O_2$  only drops slightly because there is excess air while all of the fuel is consumed. The concentration of  $NO$  can be seen to grow from the pre-heat region and into the reaction layer, but remains at a constant value due to quenching that was discussed early. Since the reaction constants are of such low magnitude in the post flame region, all species reach their final concentrations.  $NO_x$  species,  $NO$ ,  $NO_2$ , and  $N_2O$ , are formed through the reactions between several species that contain nitrogen through the combustion process. In this study, all of the nitrogen based species that go into the production of  $NO_x$  were considered. All of the nitrogen based species have very low concentrations in the flame. Their presence do not effect the production of higher concentration species, such as,  $H_2O$  or  $CO_2$ . The comparison of concentration of the major species against the nitrogen based species can be seen in figure 2 and figure 3.

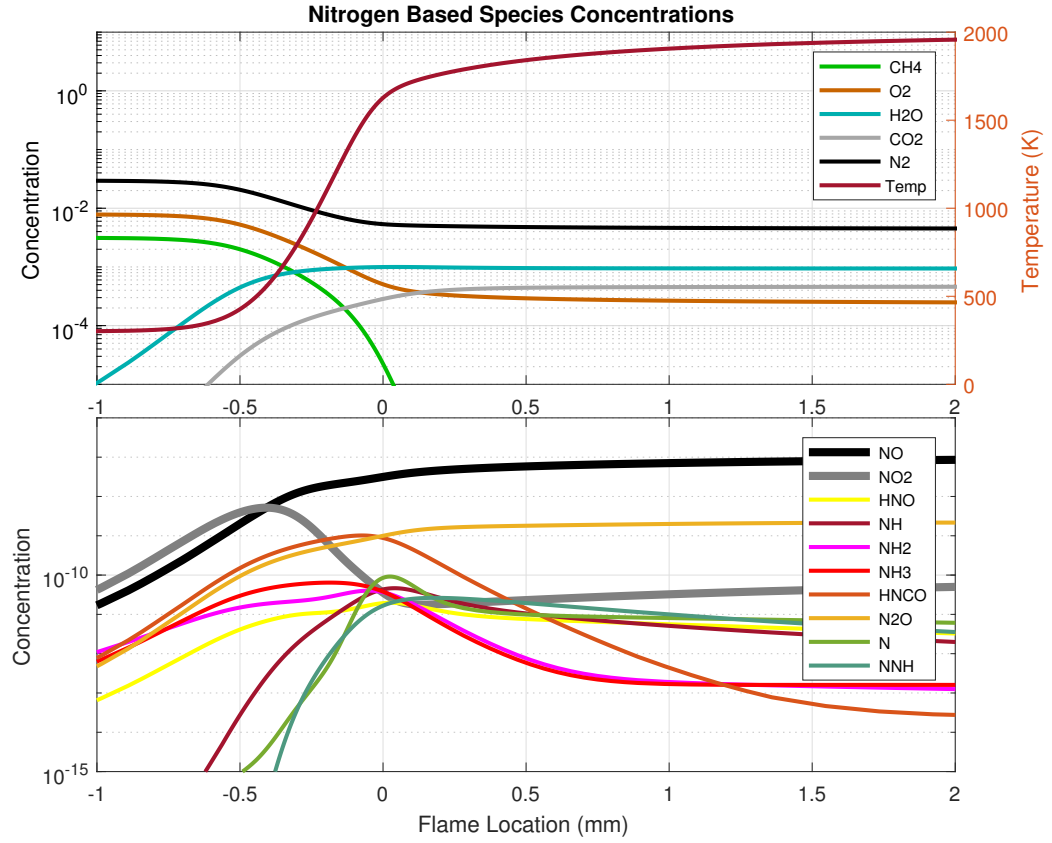


Figure 2: More Prominent Nitrogen Based Species Concentrations

From figure 2 and 3, it is obvious to see that the nitrogen based species are at least eight orders of magnitude smaller in concentration when compared to the major species. Therefore, although these low concentration species can react to produce the higher concentration species, it is at such low concentrations that their contribution can be considered negligible.

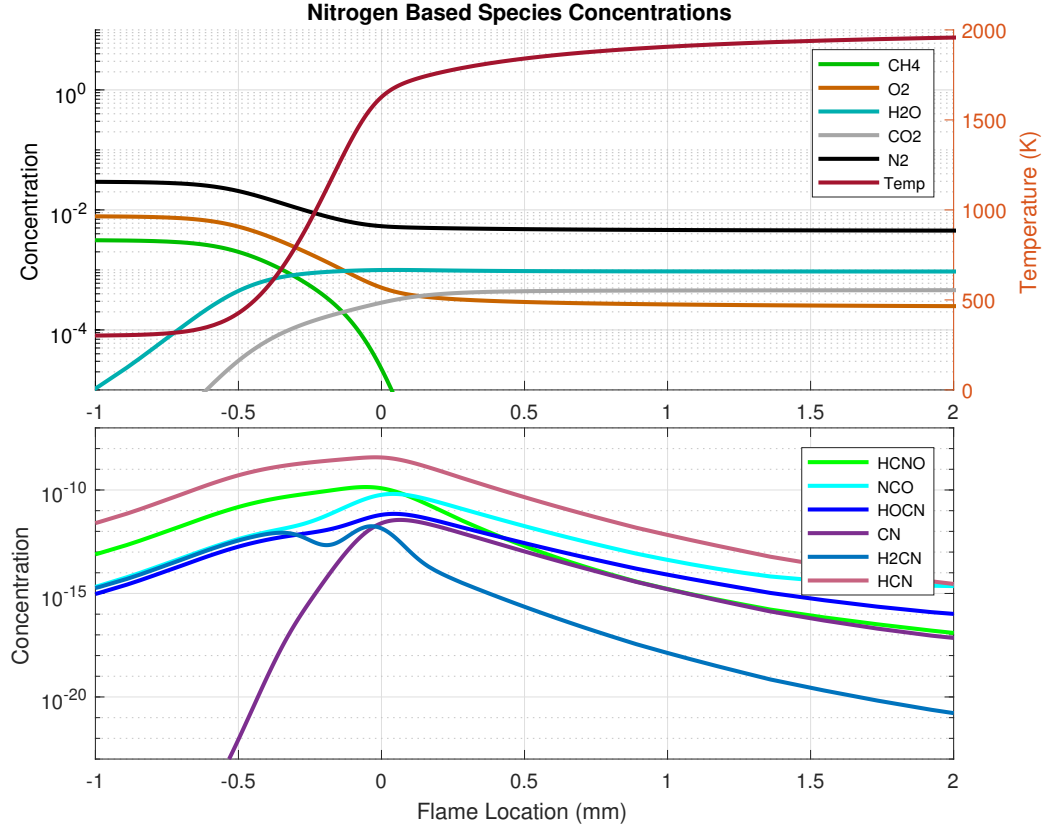


Figure 3: Less Prominent Nitrogen Based Species Concentrations

The main nitrous oxide species,  $N_2O$ ,  $NO$  and  $NO_2$ , are among the highest concentration for  $NO_x$  species. Although the concentrations are still numerous orders of magnitude lower, only 100 parts per billion are needed to cause adverse health effects to the respiratory system.

### 3.2 Mechanism Comparison

Now, choosing the best reaction mechanism for this research was the first major obstacle. GRI-Mech 3.0, developed at the University of California Berkeley, was chosen as the base mechanism used for the numerical flame analysis. GRI-Mech 3.0 contains both the main species in combustion as well as the nitrogen based species desired for this study. A second mechanism was necessary in order to reinforce our results. Since the goal of this research was to reduce the number of reactions, a simplified GRI-Mech 3.0 mechanism developed by Dr. Tianfeng Lu at the University of Connecticut, was chosen to see if his reductions could immediately be applied [23]. Although Dr. Lu's mechanism reduced the number of reactions and species from the original GRI-Mech 3.0 mechanism, he did not consider Nitrogen based species due to their extremely low concentrations in the flame. Therefore, a Nitrogen based mechanism was taken from the University of San Diego and was combined with Dr. Lu's simplified GRI-Mech 3.0 mechanism. Again, there was no error in doing this because the low concentration reactions from the nitrogen mechanism has no effect on the major species. The newly formed mechanism was then simulated through Cantera to provide flame data.

In order to compare the two mechanisms to see their similarities, their flame speeds were plotted for different equivalence ratios as seen in figure 4.

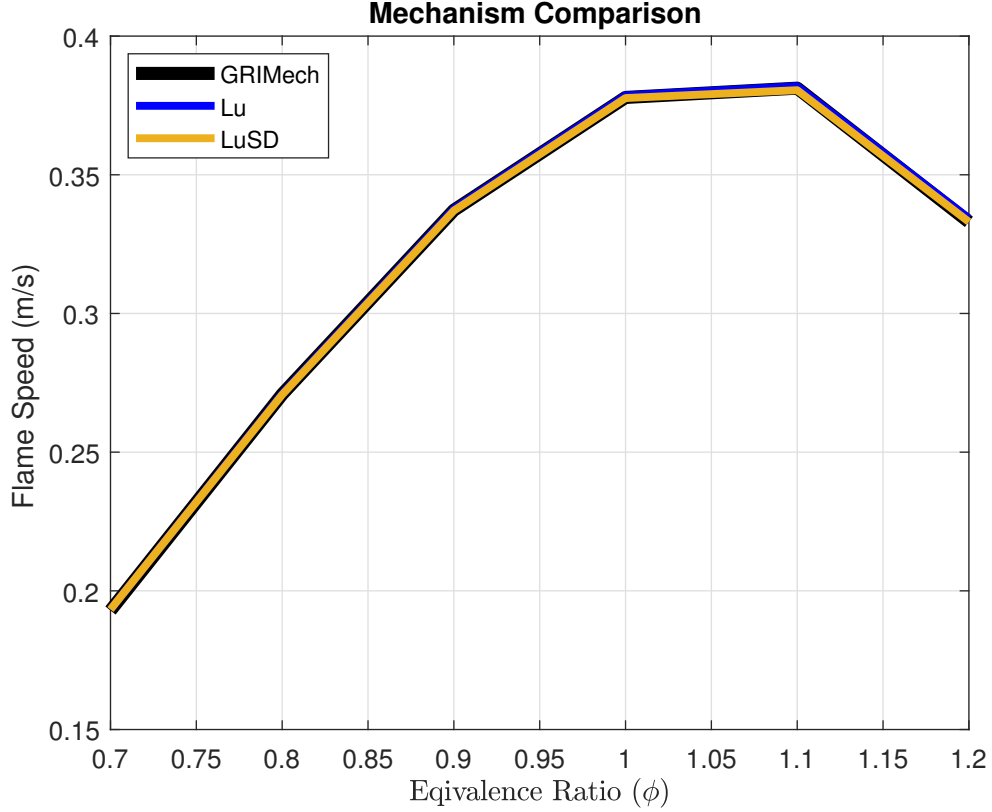


Figure 4: Comparison of GRI-Mech 3.0, Lu, and Lu + SD

The flame velocity calculated for each mechanism is consistent with the experimental flame velocities for a premixed, methane-air flame. [18] Now, analyzing the graph, the addition of the Nitrogen based UCSD mechanism had no effect on the structure of the flame. Also, the comparison of GRI-Mech 3.0, Lu, and Lu + SD mechanisms all share the same flame speed for each equivalence ratio. Since the flame speeds were equivalent, the next comparison was the radical concentrations. The radicals chosen for comparison;  $OH$ ,  $O$ , and  $H$  were chosen due to their importance in causing reactions to occur in the flame. The comparison of these major species can be seen in figure 5.



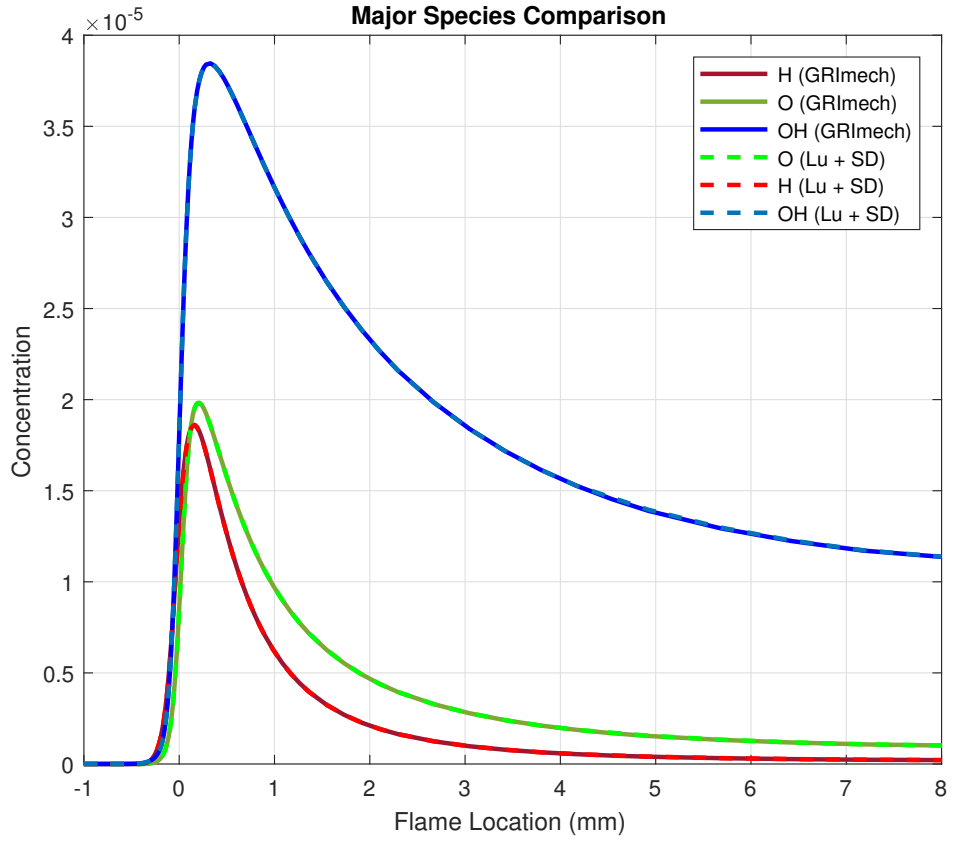


Figure 5: Comparison of Radicals Between GRI-Mech 3.0 and Lu + SD Mechanisms

The radical concentrations from both GRI-Mech 3.0 and Lu + SD mechanisms are equivalent. Therefore, the mechanisms seem to be interchangeable, but when comparing the Nitrogen based species between the two mechanisms, there are clear differences.

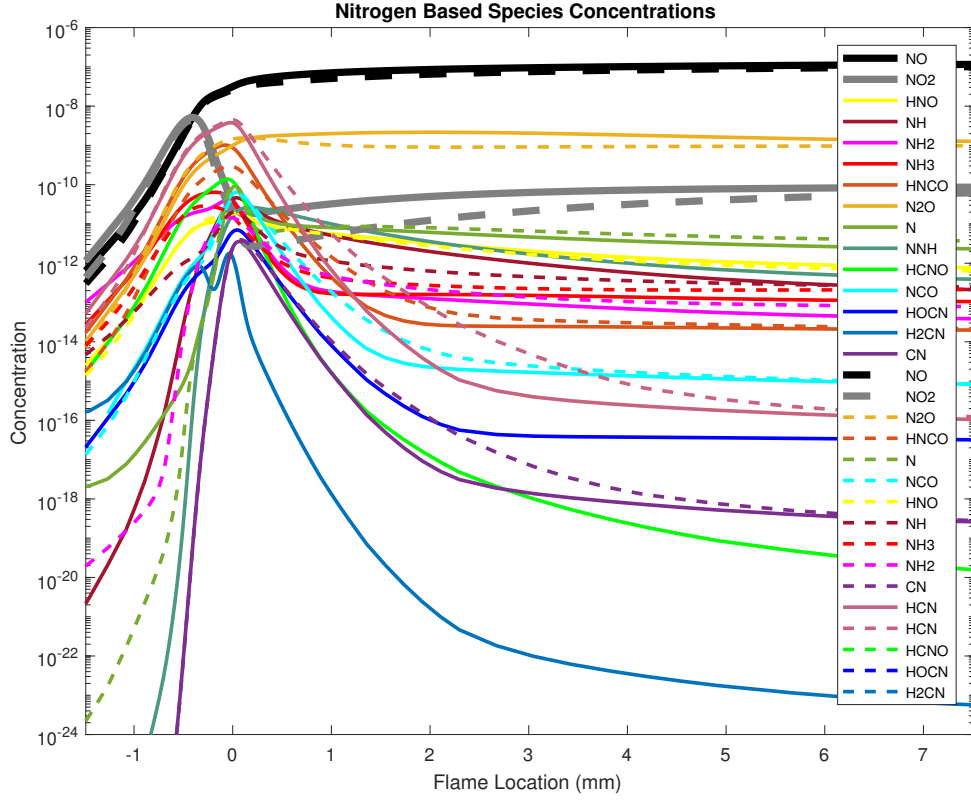


Figure 6: Comparison of Nitrogen Based Species Between GRI-Mech 3.0 and Lu + SD

The solid lines are the concentration of the nitrogen based species from GRI-Mech 3.0 while the dashed lines are the concentration of the nitrogen based species from the Lu mechanism combined with the nitrogen mechanism from UCSD. The reason that these low concentration species are different between the two mechanisms is because when Dr. Lu reduced the GRI-Mech 3.0 mechanism he removed several low concentration species and reactions. Since this study is based on low concentration Nitrogen species, the species and reactions removed by Dr. Lu have important roles in the production and consumption of all the species shown in figure 6. Therefore, we can not accurately compare GRI-Mech 3.0 and Lu + SD mechanisms. The GRI-Mech 3.0 mechanism was chosen to be used for the remainder of the study.

### 3.3 Mechanism Analysis

Now that the GRI-Mech 3.0 mechanism has been chosen as the best mechanism for this study, its contents can be discussed. The GRI-Mech 3.0 mechanism contains 325 reactions between 53 species. The list of these species can be found in the list below.

#### 1. Mechanism Species

- |         |            |             |          |
|---------|------------|-------------|----------|
| • $H_2$ | • $OH$     | • $C$       | • $CH_3$ |
| • $H$   | • $H_2O$   | • $CH$      | • $CH_4$ |
| • $O$   | • $HO_2$   | • $CH_2$    | • $CO$   |
| • $O_2$ | • $H_2O_2$ | • $CH_2(S)$ | • $CO_2$ |

• $HCO$	• $C_2H_6$	• $NO_2$	• $NCO$
• $CH_2O$	• $HCCO$	• $N_2O$	• $N_2$
• $CH_2OH$	• $CH_2CO$	• $HNO$	• $Ar$
• $CH_3O$	• $HCCOH$	• $CN$	• $C_3H_7$
• $CH_3OH$	• $N$	• $HCN$	• $C_3H_8$
• $C_2H$	• $NH$	• $H_2CN$	• $CH_2CHO$
• $C_2H_2$	• $NH_2$	• $HCNN$	• $CH_3CHO$
• $C_2H_3$	• $NH_3$	• $HCNO$	
• $C_2H_4$	• $NNH$	• $HOCN$	
• $C_2H_5$	• $NO$	• $HNCO$	

It can be seen from the list of species in the mechanism that there are 18 Nitrogen based species that contribute to the creation and destruction of  $NO$  and  $NO_2$ . Although these species make up a significant portion of the mechanism, referring back to figure 3 and 4, it is obvious that their concentrations are much lower than main species and radical concentrations. Now that different sections of the flame have been defined, the behavior of the  $NO_x$  species in each region can be analyzed. As the species progress through the flame from the pre-heat region to the post-flame region, their concentrations are continuously changing. This change is do to the reactions in which a given species is involved, whether the species is being produced or consumed. Both types of reactions can be analyzed separately for each nitrogen based species. In order to determine which reactions are most important for a certain point in the flame, the Arrhenius equation is considered, where the magnitude of the reaction rate constant for a certain reaction describes the order of that reaction's importance. These reaction rate constants are constantly changing throughout the flame. An example of these distributions can be seen in figures 3 and 4 where the x-axis is the flame location in relation to the reaction layer while the y-axis is calculated using equations 32 and 33.

$$DevConsRate = 100 * \frac{NetConsRate - TotalConsRate}{NetConsRate} \quad (32)$$

$$DevProdRate = 100 * \frac{NetProdRate - TotalProdRate}{NetProdRate} \quad (33)$$

which calculates the percent a chosen reaction rate contributes when compared to the magnitude of the summation of all the reaction rates in the mechanism. Therefore, if the production or consumption of a certain species is only dependent on two reactions then the sum of the two on the graph would equal approximately 100%.

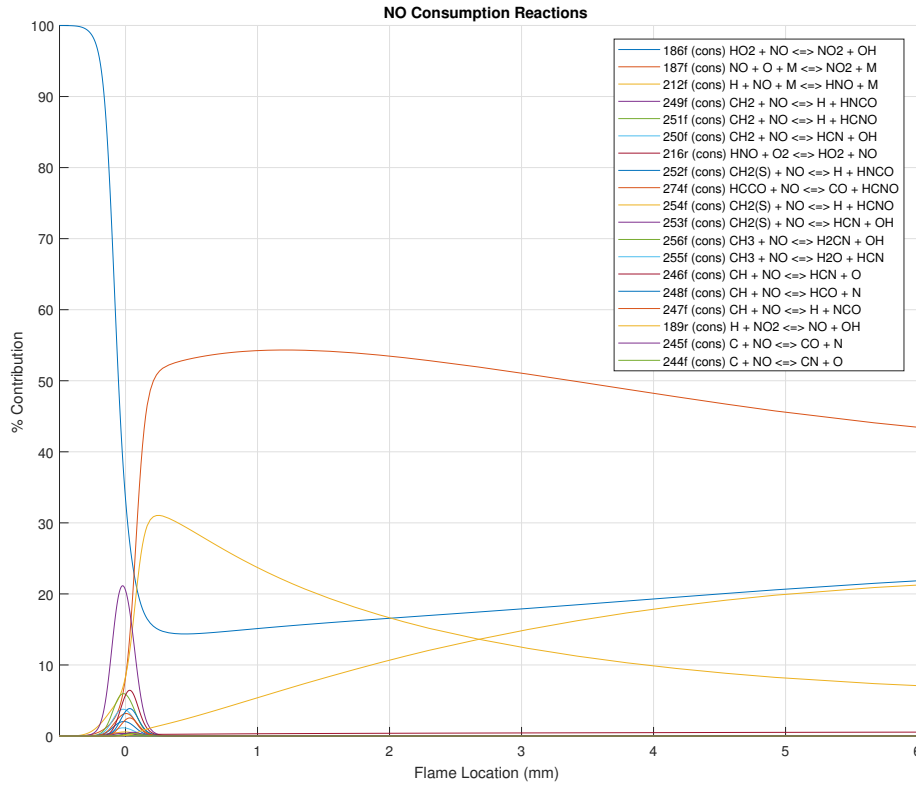


Figure 7: NO Consumption Reactions

When analyzing the percent contributions of each reaction, it can be seen that numerous reactions are needed to reach 100% in the reaction layer for both production and consumption. The post flame region for the consumption reactions are mostly defined by four reactions while the production of *NO* needs upwards of 10 to 20.

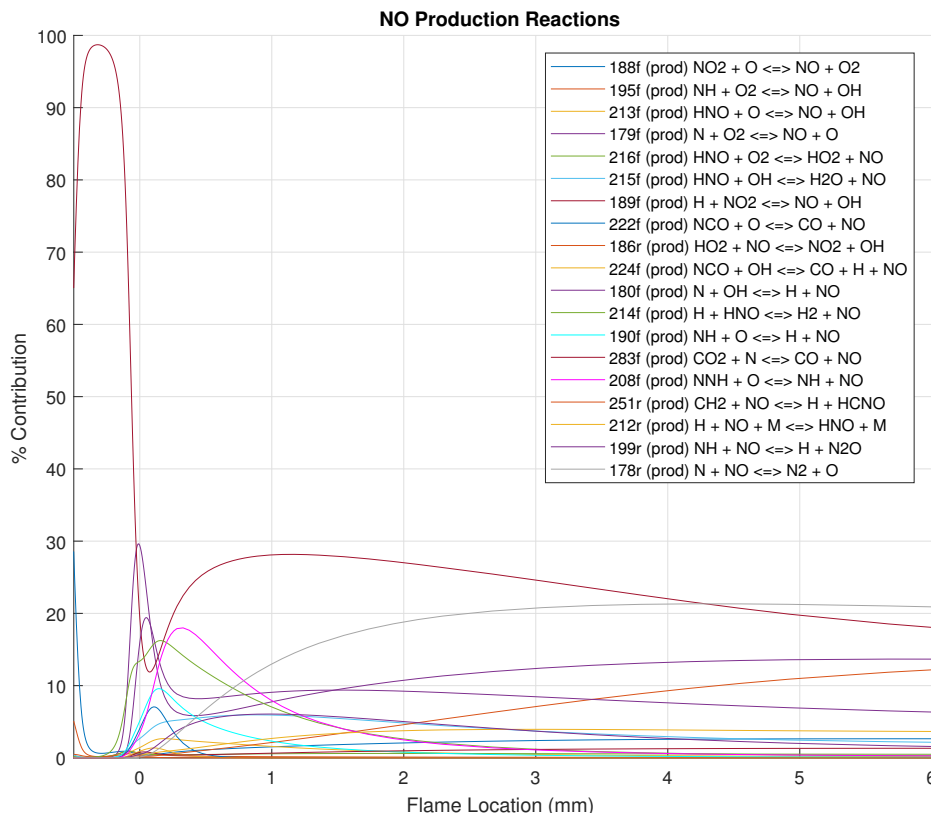


Figure 8: NO Production Reactions

It can also be seen that reactions switch importance throughout the flame. These points can be defined as 'transition points' and they occur frequently, especially in a complex species like  $NO$ . In this study, reducing the number of reactions without sacrificing accuracy is the main goal so three benchmarks were established. These benchmarks were to maintain 90%, 95%, and 99% accuracy when reducing the mechanism. In order to achieve these benchmarks, each point of the flame was analyzed to discover how many reactions are needed to be kept to reach each benchmark. Since the number of reactions that needed to be kept changes throughout the flame, each of these locations can be defined as a 'critical point'. For the sake of visualizing these changes, surface plots were generated. These plots describe the percent error depending on the flame location as well as the number of reactions kept. Each surface plot decays to zero as the number of reactions kept increases because the code eventually considers all the reactions involved. An example of these surface plots for  $NO$  can be seen in figure 9 and 10.

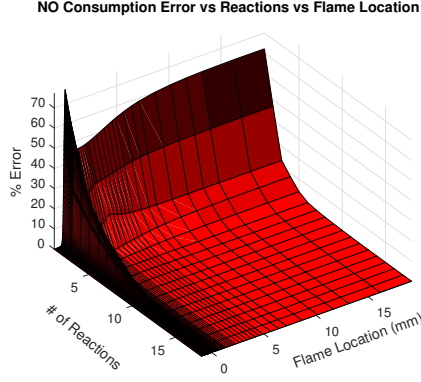


Figure 9: NO Consumption Surface Plot

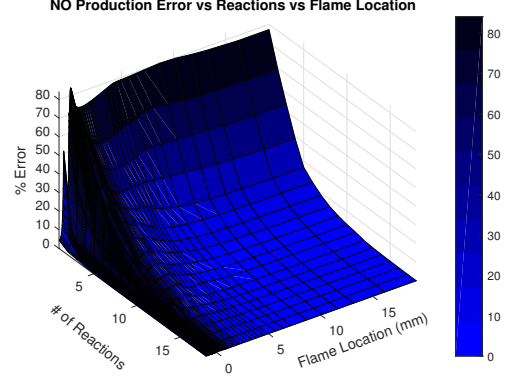


Figure 10: NO Production Surface Plot

In favor of simplicity, these surface graphs were converted into contour plots. These plots contain contour lines that display the percent error for each point of the flame as a function of the number of kept reactions. Therefore, the 10%, 5%, and 1% lines represent 90%, 95%, and 99% accuracy for the chosen species. An example of these contour plots generated from the *NO* surface plots can be seen in figure 11 and 12.

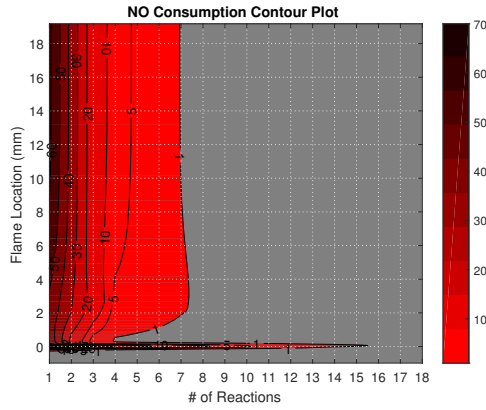


Figure 11: NO Consumption Contour Plot

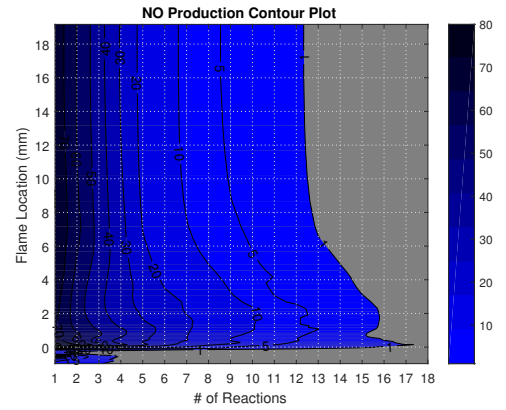


Figure 12: NO Production Contour Plot

Several reactions must be kept to achieve the set benchmarks for *NO*, but the majority of the remaining nitrogen based species in the mechanism are much simpler. The spike of required reactions in the reaction layer was expected as that is where the majority of reactions occur in the flame.

Now that the number of required reactions needed to reach the benchmarks have been found, the reactions themselves must be defined. In the same way the plots that showed the percent contribution of each reaction was generated, MatLab was used to generate a matrix of strings. This matrix listed the most important reactions to the least important reactions for each point in the flame. Now, applying the number of reactions needed at each point in the flame to reach the set benchmarks to the matrix developed, a list of reactions needed can be generated. Then, all the lists of required reactions for each species required to meet each benchmark can be compiled to a master list of which reactions are

needed to describe the formation of  $NO_x$ . Therefore, the reactions not on the list can be removed without sacrificing unknown amounts of accuracy.

### 3.4 Steady State

Another way to simplify the flame mechanisms for turbulent flame simulations is to investigate if the steady state approximation can be applied to any of the Nitrogen based species. The steady state approximation can be applied when the magnitude of the production and consumption of a species is much larger than its transport properties, comprised of the advective and diffusive terms, therefore, the difference between the production and consumption terms is nearly 0. Hence, the reason this is called a steady state 'assumption' because it comes with interpretation from the researcher through quantitative analysis. In the past, the steady state approximation has mostly been used in a qualitative way. When this assumption is found to be valid, the steady state species are being created and destroyed so fast that the advective and diffusive terms can be said to not have any influence. In other words, the steady state species are being created and destroyed before they progress any farther in the flame. Therefore, there is no need for their advective and diffusive terms to be calculated at any point in the flame. Referring back to figure 1, the x-axis represents the transport while the y-axis represents the concentration of the species. At any point in the flame the change in the y-direction is the only occurrence for a steady state species. Now, examining the transport equation defined as

$$\frac{\delta}{\delta x_j}(\rho u_j Y_i) - \frac{\delta}{\delta x_j} \left( \rho D_i \frac{\delta Y_i}{\delta x_j} \right) = Production[Y_i] - Consumption[Y_i] \quad (34)$$

where the first term is the advective term and the second is the diffusive term. When the steady state assumption is applied, the production reactions can be set equal to the consumption reactions. This process simplifies the derivation of rate laws of many step reactions because the convective and diffusive terms can be neglected. Application of the steady state approximation to a certain species can be seen in the methods section. Now, revisiting the steady state approximation, each species can be determined to be in a steady state condition throughout the flame using the following equation

$$DevSteadyState = 100 * \frac{NetProdRate - NetConsRate}{NetConsRate} \quad (35)$$

which calculates the percent deviation out of steady state a species is at each point in the flame. If this deviation is nearly zero, then the steady state condition can be applied to that chosen species. In order to illustrate how this assumption is applied, consider the nitrogen based species  $CN$ .  $CN$  is a steady state species, which can be seen from figure 13. Even though  $CN$  deviates from steady state slightly around the reaction layer, the assumption can still be applied. Again, it is the researcher's discretion as to if the assumption can be applied. In this study, a 1% deviation is well within the bounds to apply the steady state assumption. Conversely, for a species like  $HCN$ , the steady state approximation cannot be applied because it deviates as much as 90% in the reaction layer through the post flame as seen in figure 14.

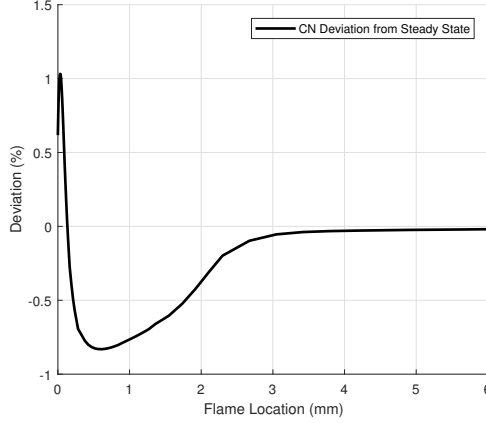


Figure 13:  $CN$  Steady State Approximation

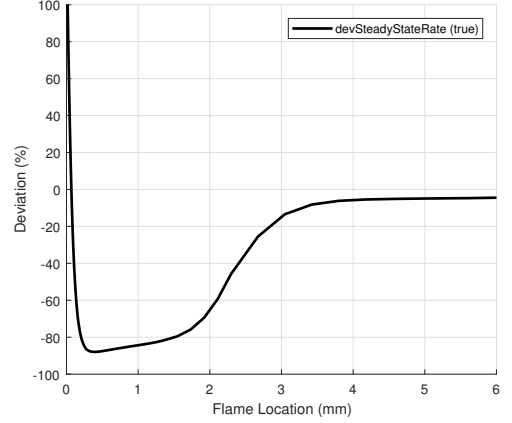


Figure 14:  $HCN$  Steady State Approximation

Now that  $CN$  has been proven to be a steady state species, the production and consumption reactions of  $CN$  can be found from the entirety of the flame. These reactions are shown in table 1 and 2. The 'f' and 'r' attached to the end of the reaction rate number dictates the direction of the reaction. Since these reactions are reversible, the 'f' represents the reaction in the forward direction, from left to right, and the 'r' represents the reaction in the reverse direction, from left to right.

Table 1:  $CN$  Consumption Reactions

$CN$ Consumption Reactions		
#	Mech #	Reaction
1	220f	$CN + O_2 \leftrightarrow NCO + O$
2	221f	$CN + H_2 \leftrightarrow HCN + H$
3	219f	$CN + H_2O \leftrightarrow HCN + OH$
4	218f	$CN + OH \leftrightarrow NCO + H$
5	217f	$CN + O \leftrightarrow CO + N$
6	233r	$HCN + O \leftrightarrow CN + OH$

Table 2:  $CN$  Production Reactions

$CN$ Production Reactions		
#	Mech #	Reaction
1	219r	$CN + H_2O \leftrightarrow HCN + OH$
2	233f	$HCN + O \leftrightarrow CN + OH$
3	221r	$CN + H_2 \leftrightarrow HCN + H$
4	220r	$CN + O_2 \leftrightarrow NCO + O$
5	218r	$CN + OH \leftrightarrow NCO + H$
6	244f	$C + NO \leftrightarrow CN + O$
7	239f	$C + N_2 \leftrightarrow CN + N$

Since the steady state approximation states that



$$Production[CN] - Consumption[CN] \approx 0$$

$$\therefore Production[CN] \approx Consumption[CN]$$

which means that the production and consumption equations for  $CN$  can be related using the reaction rates and all the species involve. The relation for  $CN$  becomes

$$\begin{aligned} & [CN] \left( k_{220f}[O_2] + k_{221f}[H_2] + k_{219f}[OH] + k_{218f}[OH] + k_{217f}[O] + k_{233f}[OH] \right) \\ &= [HCN] \left( k_{219r}[OH] + k_{233f}[O] + k_{221f}[H] \right) + [NCO] \left( k_{220r}[O] + k_{218r}[H] \right) + [N_2] \left( k_{239f}[C] \right) \end{aligned}$$

which can be manipulated into a ratio of reaction rates and species involved with  $CN$  throughout the entirety of the flame. This ratio is written as

$$[CN] = \left[ \frac{[HCN] \left( k_{219r}[OH] + k_{233f}[O] + k_{221f}[H] \right) + [NCO] \left( k_{220r}[O] + k_{218r}[H] \right) + [N_2] \left( k_{239f}[C] \right)}{\left( k_{220f}[O_2] + k_{221f}[H_2] + k_{219f}[OH] + k_{218f}[OH] + k_{217f}[O] + k_{233f}[OH] \right)} \right]$$

This relation clarifies the interactions of  $CN$  throughout the flame. This ratio shows that  $CN$  is a function of the concentration of  $OH$ ,  $O$ ,  $H$ ,  $C$ ,  $O_2$ , and  $H_2$  as well as temperature, due to the rate constant being a function of temperature. Therefore, the concentration can be calculated at any point in the flame depending on the values of each of its variables.

$$[CN] = f([OH], [O], [H], [C], [O_2], [H_2], T)$$

Again, this relationship could not have been established if the species is not in a steady state. Similar to the relation developed for  $CN$ , the concentration of a species not in steady state can also be found, but they would also be a function of the advective and diffusive terms at each point of the flame. Once all of the steady state species are defined, their advective and diffusive term values can be ignored in the calculations, which will save a large amount of computing time.

## 4 Results

Now that the process for reducing the flame mechanism has been defined, it can be iterated for all 18 nitrogen based species involved in  $NO_x$  production and consumption. In this section, the two main  $NO_x$  species will be discussed:  $NO$  and  $NO_2$ . These species will be highlighted due to the fact that they are the main harmful nitrogen based species. The results from all the other nitrogen based species can be found in the Appendix.

### 4.1 NO Analysis

To start, the main  $NO_x$  species will be discussed,  $NO$ . This species is very complex in its formation because it involves several intermediate reactions and intermediate species in its consumption and production throughout the flame. First, the production of  $NO$  will be investigated. The surface and contour plots were generated as described in the methods section.

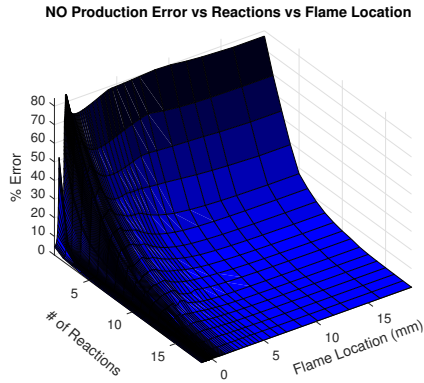


Figure 15:  $NO$  Production Surface Plot

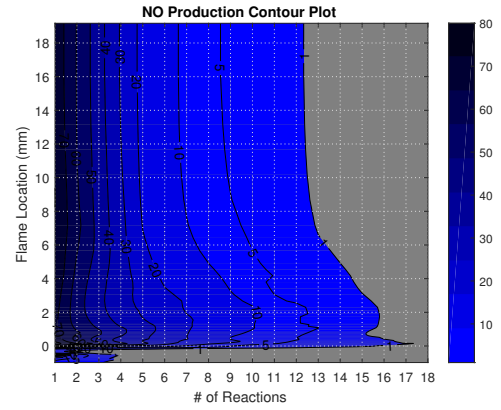


Figure 16:  $NO$  Production Contour Plot

In order to more accurately study the behavior of  $NO$ , the contour plots can be centralized over both the reaction layer and post-flame regions of the flame. After rescaling the contour plot, the location of the 'critical points' become much more clear. In order to accurately describe the production of  $NO$ , up to 18 reactions must be kept for the reaction layer while 16 must be kept for the post-flame region to achieve the 99% benchmark. The number of reactions needed to kept greatly reduces for the 90% and 95% benchmarks.

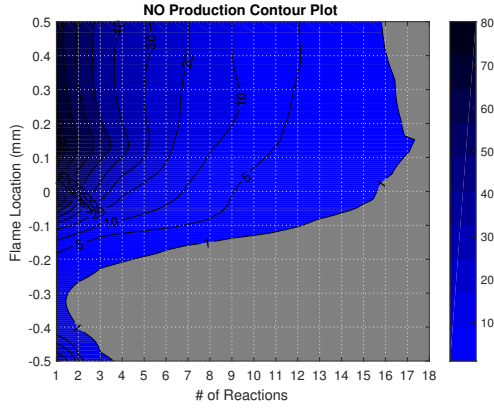


Figure 17:  $NO$  Production Reaction Layer Contour Plot

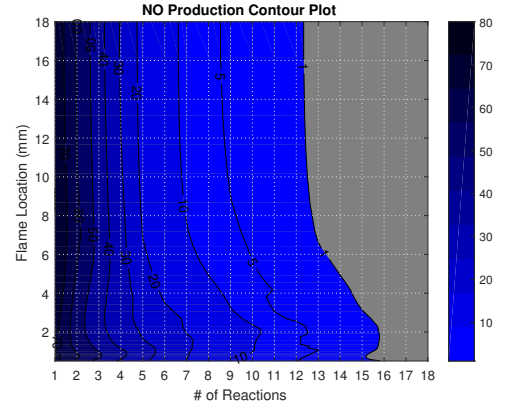


Figure 18:  $NO$  Production Post Flame Contour Plot

Now, the consumption of  $NO$  is much less complex. With the surface and contour plots generated, it can be seen that the reaction layer still requires numerous reactions to maintain the benchmarks, but the post-flame region does not.

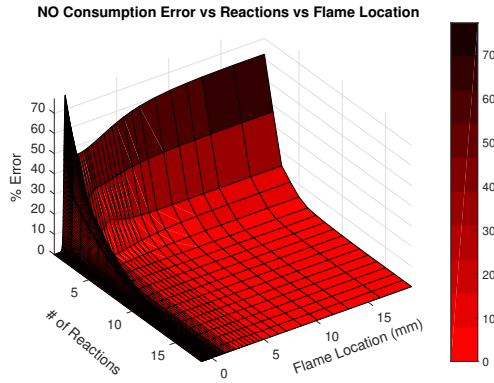


Figure 19:  $NO$  Consumption Surface Plot

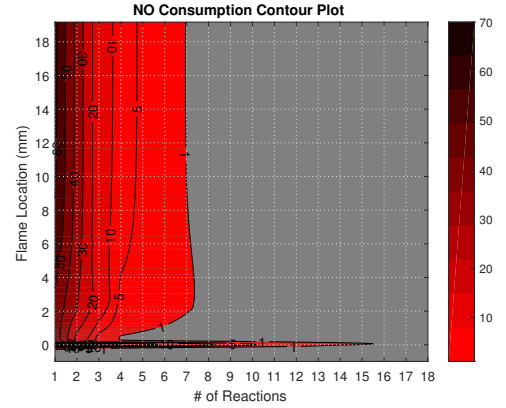


Figure 20:  $NO$  Consumption Contour Plot

Again, the contour plot is rescaled for better visualization of the reaction layer and post-flame region. The consumption of  $NO$  is most complex around the center of the reaction layer, requiring up to 16 reactions to maintain 99% accuracy while the post-flame region only requires up to 8.

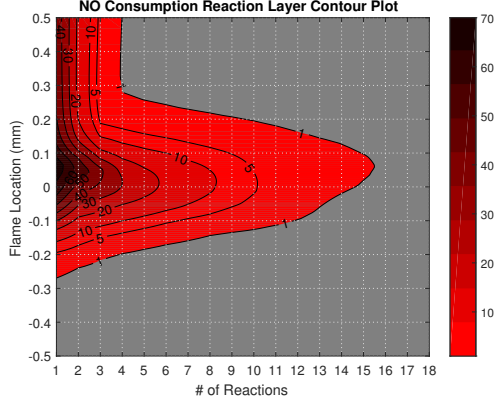


Figure 21: *NO* Consumption Reaction Layer Contour Plot

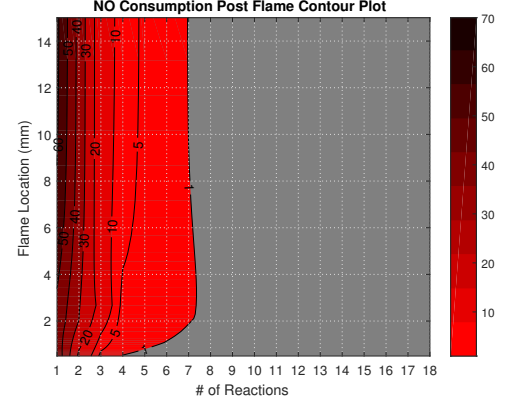


Figure 22: *NO* Consumption Post Flame Contour Plot

As stated in the methods section, now that the required number of reactions needed is known, the actual reactions need to be defined. By using the matrix of reactions in order of importance and the flame locations, the following tables can be developed to state which reactions must be kept for each of the three flame regions for production and consumption.

Table 3: *NO* Consumption Pre-Heat Region

Consumption Pre-Heat Region				
#	90%	95%	99%	Reaction
1	186f	186f	186f	$HO_2 + NO \leftrightarrow NO_2 + OH$

When analyzing the pre-heat region of the flame, it can be seen that *NO* is only consumed through one reaction, but the rate is essentially negligible. The reaction layer is the only place in the flame with high enough temperature to cause a significant reaction rate of *NO*, therefore the number of reactions for the consumption of *NO* increases from 1 up to 17 for the 99% accuracy benchmark.

Table 4: *NO* Consumption Reaction Layer

Consumption Reaction Layer				
#	90%	95%	99%	Reaction
1	186f	186f	186f	$HO_2 + NO \leftrightarrow NO_2 + OH$
2	212f	212f	212f	$H + NO + M \leftrightarrow HNO + M$
3	249f	249f	249f	$CH_2 + NO \leftrightarrow H + HNC O$
4	187f	187f	187f	$NO + O + M \leftrightarrow NO_2 + M$
5	251f	251f	251f	$CH_2 + NO \leftrightarrow H + HCNO$
6	250f	250f	250f	$CH_2 + NO \leftrightarrow OH + HCN$
7	274f	274f	274f	$HCCO + NO \leftrightarrow HCNO + CO$
8	246f	246f	246f	$CH + NO \leftrightarrow HCN + O$
9	248f	248f	248f	$CH + NO \leftrightarrow N + HCO$
10	247f	247f	247f	$CH + NO \leftrightarrow H + NCO$
11	-	252f	252f	$CH_2(S) + NO \leftrightarrow H + HNC O$
12	-	189r	189r	$NO_2 + H \leftrightarrow NO + OH$
13	-	-	255f	$CH_3 + NO \leftrightarrow HCN + H_2O$
14	-	-	245f	$C + NO \leftrightarrow CO + N$
15	-	-	253f	$CH_2(S) + NO \leftrightarrow OH + HCN$
17	-	-	244f	$C + NO \leftrightarrow CN + O$

When comparing the reactions that are needed to be kept between the reaction layer and the post flame regions, trends can be assessed. Reactions 187f, 212f, 186f, and 189r are prominent in both regions, but reactions 249f, 251f, 250f, 274f, 246f, 248f, 247f, 252f, 255f, 245f, 253f, and 244f are only prominent in the reaction layer. As we progress to the post-flame region, the reaction rates of these reactions are such a small magnitude compared to the other reactions that they are considered to be negligible. This results in reactions 216r, 180r, 188r, 179r, and 215r as being reactions that are most crucial.

Table 5: *NO* Consumption Post Flame

Consumption Post Flame Region				
#	90%	95%	99%	Reaction
1	187f	187f	187f	$NO + O + M \leftrightarrow NO_2 + M$
2	212f	212f	212f	$H + NO + M \leftrightarrow HNO + M$
3	186f	186f	186f	$HO_2 + NO \leftrightarrow NO_2 + OH$
4	189r	189r	189r	$NO_2 + H \leftrightarrow NO + OH$
5	-	-	216r	$HNO + O_2 \leftrightarrow HO_2 + NO$
6	-	-	180r	$N + OH \leftrightarrow NO + H$
7	-	-	188r	$NO_2 + O \leftrightarrow NO + O_2$
8	-	-	179r	$N + O_2 \leftrightarrow NO + O$
9	-	-	215r	$HNO + OH \leftrightarrow NO + H_2O$

The trends of the reactions throughout the flame can be seen in figures 23 and

24 where the x-axis is the distance from the center of the reactions layer and the y-axis describes the percent contribution each individual reaction has to the whole mechanism for  $NO$ . The trends stated before are illustrated in these figures, where it can be seen that reactions 249f, 251f, 250f, 274f, 246f, 248f, 247f, 252f, 255f, 245f, 253f, and 244f are prominent in the reaction layer, but decay to 0 as the graph progresses to the post-flame. Conversely, it can be seen that reactions 216r, 180r, 188r, 179r, and 215r begin to increase in importance in the post-flame region. Finally, reactions 187f, 212f, 186f, and 189r do not dissipate throughout the entirety of the flame, therefore, these reactions are constantly occurring in the consumption process of  $NO$ .

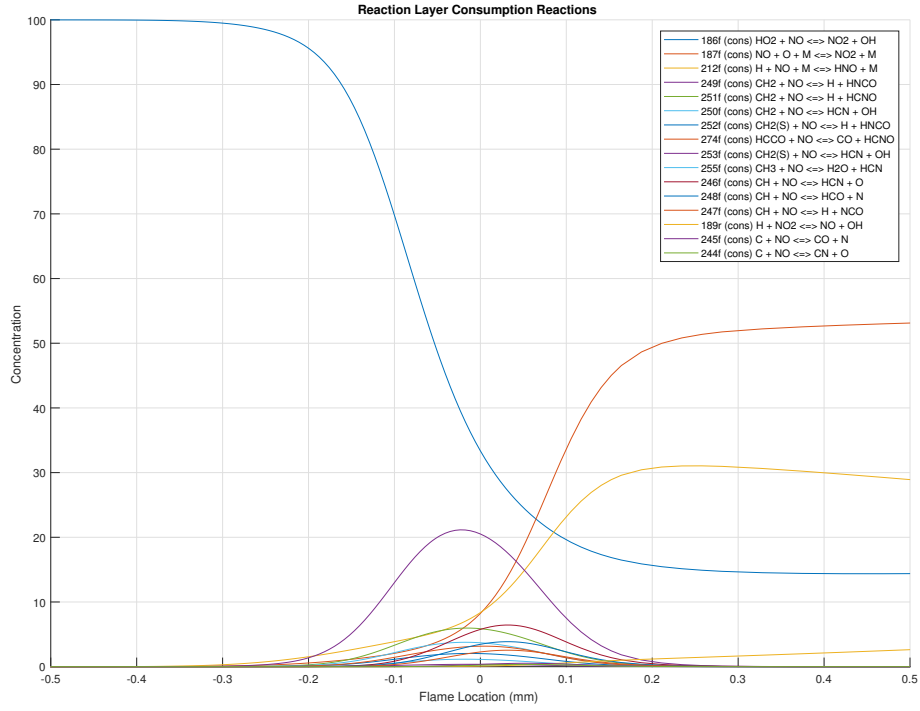


Figure 23: NO Consumption Reactions

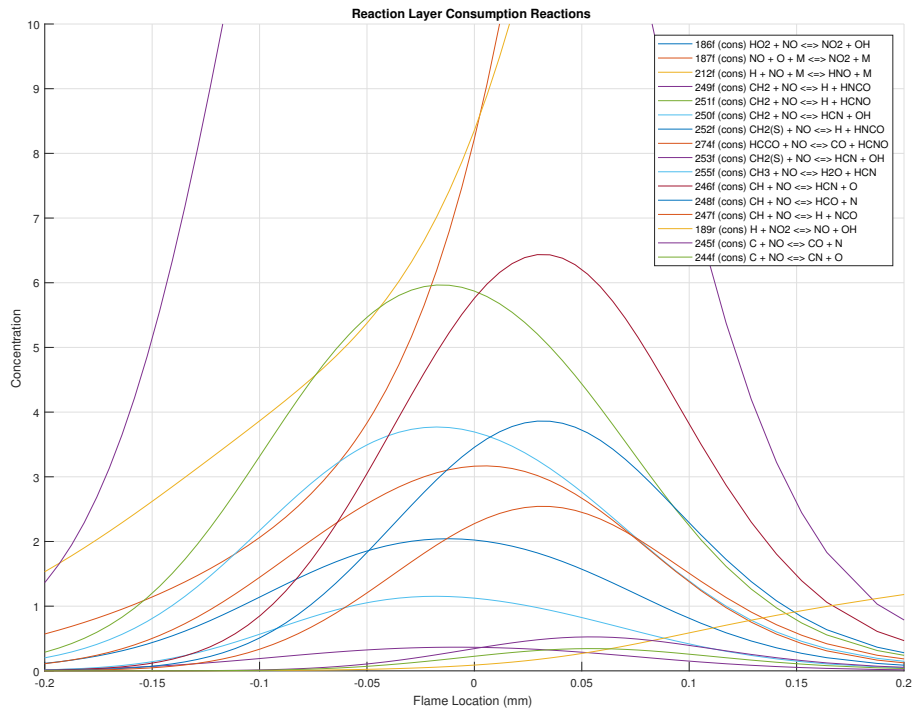


Figure 24: NO Consumption Reactions Enlarged

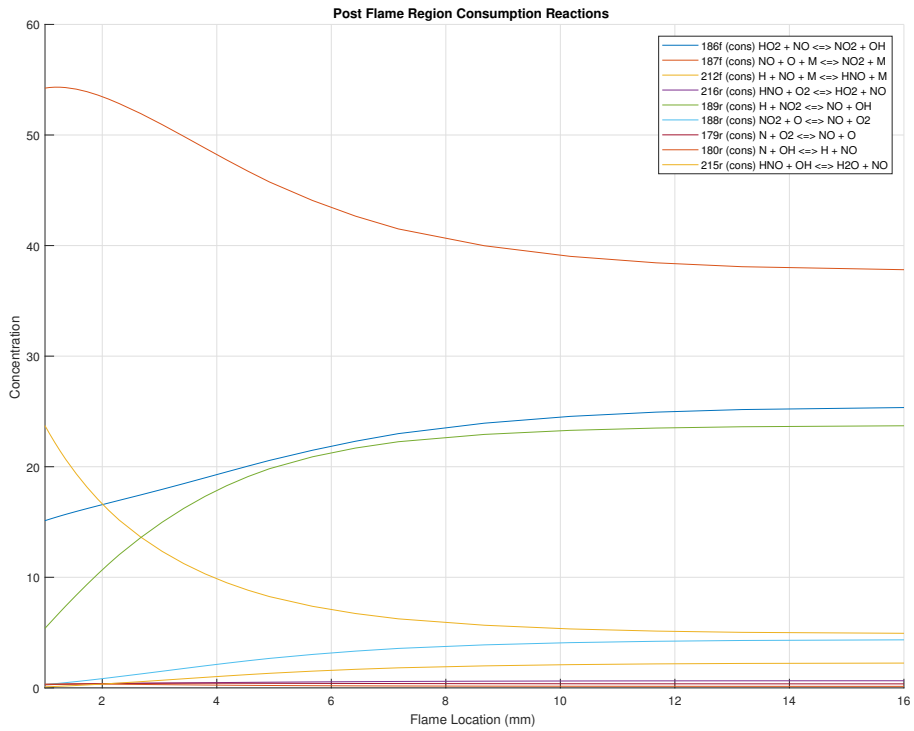


Figure 25: NO Consumption Reactions

Now that the consumptions reactions have been analyzed, the same process can

be applied to the production reactions. In contrast to the consumption of  $NO$ , there several reactions present in the preheat region that describe the production of  $NO$ .

Table 6:  $NO$  Production Pre-Heat Region

Production Pre-Heat Region				
#	90%	95%	99%	Reaction
1	188f	188f	188f	$NO_2 + O \leftrightarrow NO + O_2$
2	195f	195f	195f	$NH + O_2 \leftrightarrow NO + OH$
3	213f	213f	213f	$HNO + O \leftrightarrow NO + OH$
4	179f	179f	179f	$N + O_2 \leftrightarrow NO + O$
5	189f	189f	189f	$NO_2 + H \leftrightarrow NO + OH$
6	-	-	215f	$HNO + OH \leftrightarrow NO + H_2O$
7	-	-	186r	$HO_2 + NO \leftrightarrow NO_2 + OH$

When comparing the pre-heat region and the reaction layer, it can be seen that all the reactions that begin to produce  $NO$ , continue to do so into the reaction layer. Since the temperature rises in the reaction layer, more reactions must become apparent and have to be accounted for as well.

Table 7:  $NO$  Production Reaction Layer

Production Reaction Layer				
#	90%	95%	99%	Reaction
1	189f	189f	189f	$NO_2 + H \leftrightarrow NO + OH$
2	188f	188f	188f	$NO_2 + O \leftrightarrow NO + O_2$
3	195f	195f	195f	$NH + O_2 \leftrightarrow NO + OH$
4	214f	214f	214f	$HNO + H \leftrightarrow H_2 + NO$
5	216f	216f	216f	$HNO + O_2 \leftrightarrow HO_2 + NO$
6	179f	179f	179f	$N + O_2 \leftrightarrow NO + O$
7	180f	180f	180f	$N + OH \leftrightarrow NO + H$
8	190f	190f	190f	$NH + O \leftrightarrow NO + H$
9	222f	222f	222f	$NCO + O \leftrightarrow NO + CO$
10	208f	208f	208f	$NNH + O \leftrightarrow NH + NO$
11	215f	215f	215f	$HNO + OH \leftrightarrow NO + H_2O$
12	213f	213f	213f	$HNO + O \leftrightarrow NO + OH$
13	199r	199r	199r	$NH + NO \leftrightarrow N_2O + H$
14	178r	178r	178r	$N + NO \leftrightarrow N_2 + O$
15	-	224f	224f	$NCO + OH \leftrightarrow NO + H + CO$
16	-	283f	283f	$N + CO_2 \leftrightarrow NO + CO$
17	-	212f	212f	$H + NO + M \leftrightarrow HNO + M$
18	-	182f	182f	$N_2O + O \leftrightarrow 2NO$
19	-	-	186r	$HO_2 + NO \leftrightarrow NO_2 + OH$

Similarly, there are several reactions that are still crucial to the production of



$NO$  from the reaction layer that are also needed in the post flame. Despite these reactions making up the majority of the contribution, in order to reach the desired benchmarks of 90%, 95%, and 99%, numerous reactions that contribute 5% or less must be kept.

Table 8:  $NO$  Production Post Flame

Production Post Flame				
#	90%	95%	99%	Reaction
1	189f	189f	189f	$NO_2 + H \leftrightarrow NO + OH$
2	208f	208f	208f	$NNH + O \leftrightarrow NH + NO$
3	214f	214f	214f	$HNO + H \leftrightarrow H_2 + NO$
4	180f	180f	180f	$N + OH \leftrightarrow NO + H$
5	178r	178r	178r	$N + NO \leftrightarrow N_2 + O$
6	179f	179f	179f	$N + O_2 \leftrightarrow NO + O$
7	215f	215f	215f	$HNO + OH \leftrightarrow NO + H_2O$
8	199r	199r	199r	$NH + NO \leftrightarrow N_2O + H$
9	190f	190f	190f	$NH + O \leftrightarrow NO + H$
10	213f	213f	213f	$HNO + O \leftrightarrow NO + OH$
11	212r	212r	212r	$H + NO + M \leftrightarrow HNO + M$
12	186r	186r	186r	$HO_2 + NO \leftrightarrow NO_2 + OH$
13	188f	188f	188f	$NO_2 + O \leftrightarrow NO + O_2$
14	182f	182f	182f	$N_2O + O \leftrightarrow 2NO$
15	-	187r	187r	$NO + O + M \leftrightarrow NO_2 + M$
16	-	283f	283f	$N + CO_2 \leftrightarrow NO + CO$
17	-	-	216f	$HNO + O_2 \leftrightarrow HO_2 + NO$

Again the trends of these reactions can be seen in figure 26 and 27 where the percent contribution is plotted against the flame location from the center of the reaction layer. These graphs illustrate the behavior of each reaction and their importance to the mechanism.

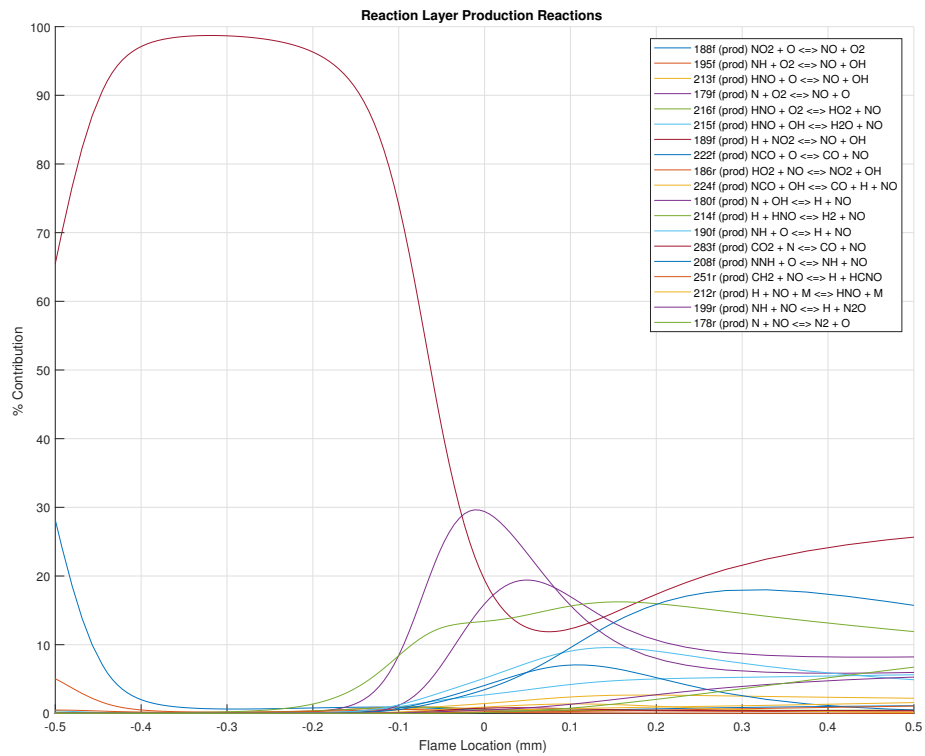


Figure 26: *NO* Reaction Layer Production Reactions

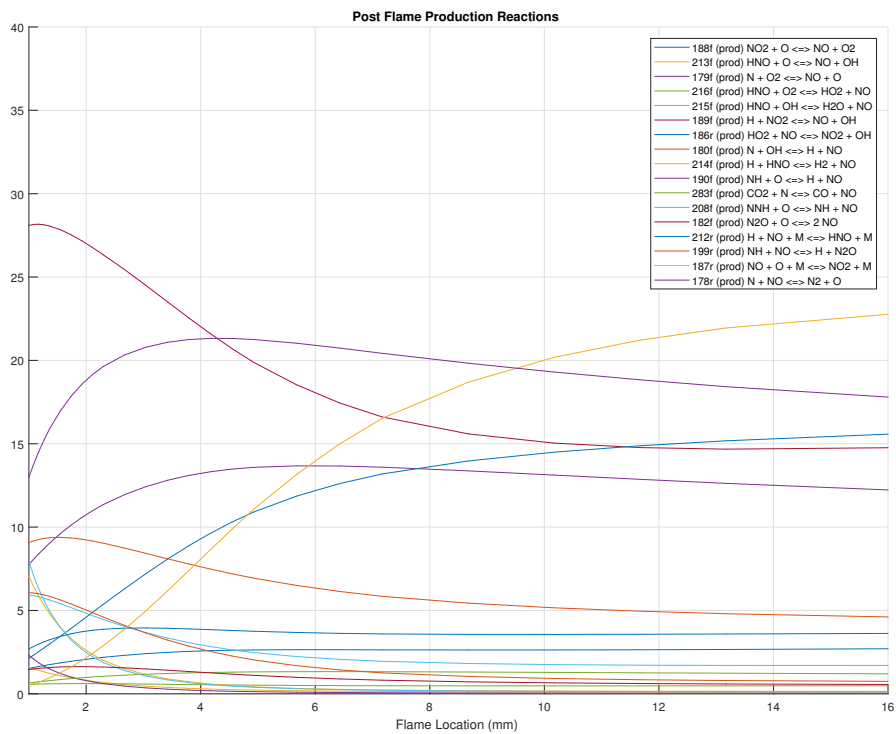


Figure 27: *NO* Post Flame Production Reactions

After the analysis of the production and consumption reactions for each flame region is completed, they can be compiled to create once cohesive list the describes the behavior of  $NO$  throughout the flame which can be seen in table 9.

Table 9:  $NO$  Required Reactions

$NO$ Required Reactions				
#	90%	95%	99%	Reaction
1	178	178	178	$N + NO \leftrightarrow N_2 + O$
2	179	179	179	$N + O_2 \leftrightarrow NO + O$
3	180	180	180	$N + OH \leftrightarrow NO + H$
4	182	182	182	$N_2O + O \leftrightarrow 2NO$
5	186	186	186	$HO_2 + NO \leftrightarrow NO_2 + OH$
6	187	187	187	$NO + O + M \leftrightarrow NO_2 + M$
7	188	188	188	$NO_2 + O \leftrightarrow NO + O_2$
8	189	189	189	$NO_2 + H \leftrightarrow NO + OH$
9	190	190	190	$NH + O \leftrightarrow NO + H$
10	195	195	195	$NH + O_2 \leftrightarrow NO + OH$
11	199	199	199	$NH + NO \leftrightarrow N_2O + H$
12	208	208	208	$NNH + O \leftrightarrow NH + NO$
13	212	212	212	$H + NO + M \leftrightarrow HNO + M$
14	213	213	213	$HNO + O \leftrightarrow NO + OH$
15	214	214	214	$HNO + H \leftrightarrow H_2 + NO$

Table 10:  $NO$  Required Reactions Continued

$NO$ Required Reactions				
#	90%	95%	99%	Reaction
16	215	215	215	$HNO + OH \leftrightarrow NO + H_2O$
17	216	216	216	$HNO + O_2 \leftrightarrow HO_2 + NO$
18	222	222	222	$NCO + O \leftrightarrow NO + CO$
19	246	246	246	$CH + NO \leftrightarrow HCN + O$
20	247	247	247	$CH + NO \leftrightarrow H + NCO$
21	248	248	248	$CH + NO \leftrightarrow N + HCO$
22	249	249	249	$CH_2 + NO \leftrightarrow H + HNCO$
23	250	250	250	$CH_2 + NO \leftrightarrow OH + HCN$
24	251	251	251	$CH_2 + NO \leftrightarrow H + HCNO$
25	274	274	274	$HCCO + NO \leftrightarrow HCNO + CO$
26	-	224	224	$NCO + OH \leftrightarrow NO + H + CO$
27	-	252	252	$CH_2(S) + NO \leftrightarrow H + HNCO$
28	-	283	283	$N + CO_2 \leftrightarrow NO + CO$
29	-	-	245	$C + NO \leftrightarrow CO + N$
30	-	-	253	$CH_2(S) + NO \leftrightarrow OH + HCN$
31	-	-	255	$CH_3 + NO \leftrightarrow HCN + H_2O$

With all of the reactions needed to produce  $NO$  defined, they can be validated by checking if the reactions from the three pathways are present. The intermediate reactions for thermal  $NO$  are the same as prompt  $NO$  and can be found in the generated list of reaction. Reactions 178, 179, and 180 are the same as equations 7, 8, and 9 respectively. These reactions are among the most influential reactions in that they contribute to the majority of  $NO$  production throughout the flame. As for the fuel-bound  $NO$  production, reaction 195 is the same as equation 28. This reaction is also one of the main contributors.

Now, to potentially reduce the mechanism for  $NO$  even further, the steady-state approximation is revisited. From figure 28, it is quite obvious that  $NO$  is not in steady state at any point in the flame. This result is expected due to the complexity of the species in which it needs several reactions to describe its production and consumption. Therefore, the software has to calculate the value of the advection and diffusion term for  $NO$  at each point in the flame.

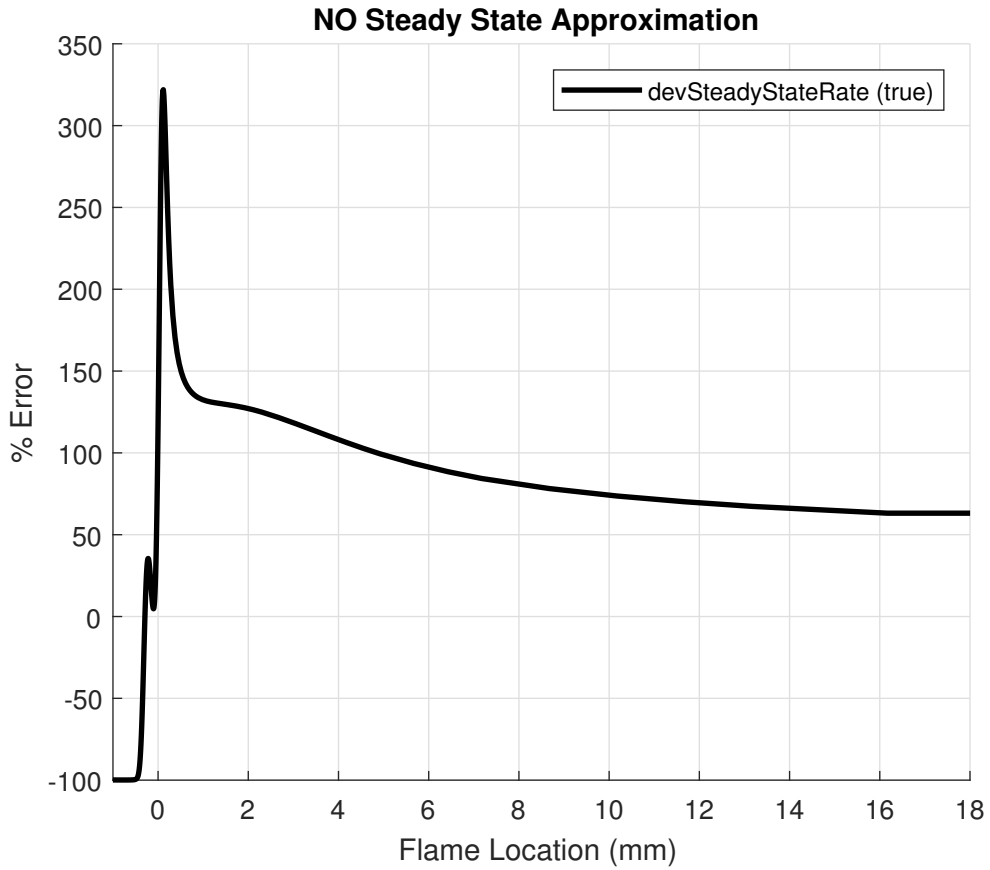


Figure 28:  $NO$  Steady State Approximation

## 4.2 $NO_2$ Analysis

Conversely to  $NO$ ,  $NO_2$  is a much less complex species. The surface and contour plots make this statement quite apparent because  $NO_2$  only needs four reactions at any point in the flame to accurately describe its production and consumption.

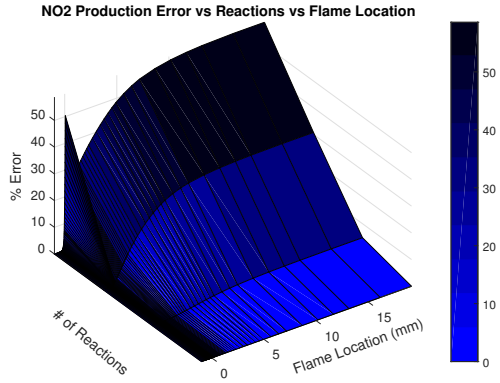


Figure 29:  $NO_2$  Production Surface Plot

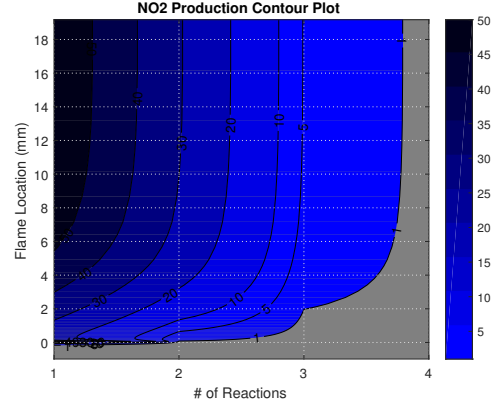


Figure 30:  $NO_2$  Production Contour Plot

The number of critical points cannot be determined from the original contour plot, but when analyzing the regional plots it can be seen that there are only two critical points for the production of  $NO_2$ .

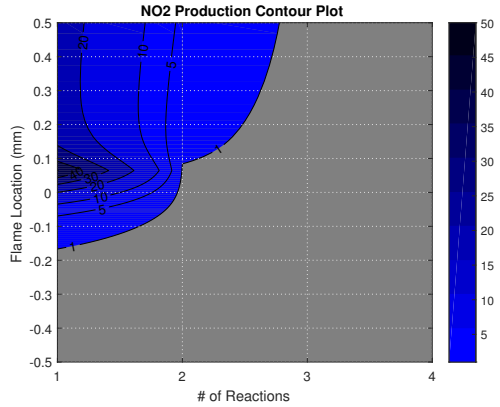


Figure 31:  $NO_2$  Production Reaction Layer Contour Plot

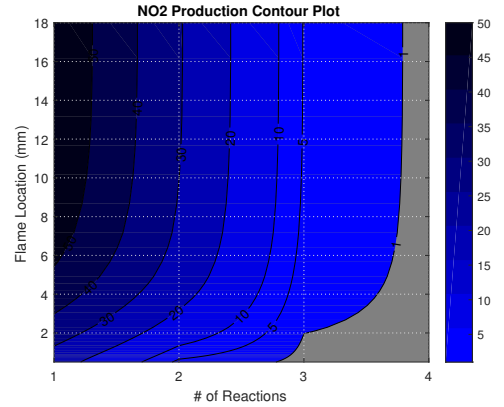


Figure 32:  $NO_2$  Production Post Flame Contour Plot

Again, the consumption surface and contour plots can be generated. When comparing both the production and consumption contour plots, they appear to be very similar because they require the same general set of reactions to describe  $NO_2$ . This generalization shows that the reactions may be in equilibrium and thus in a steady-state which will be discussed further.

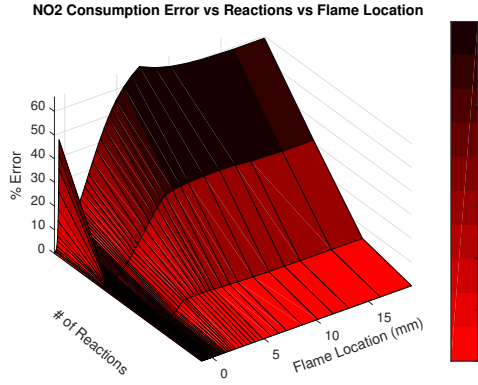


Figure 33:  $NO_2$  Consumption Surface Plot

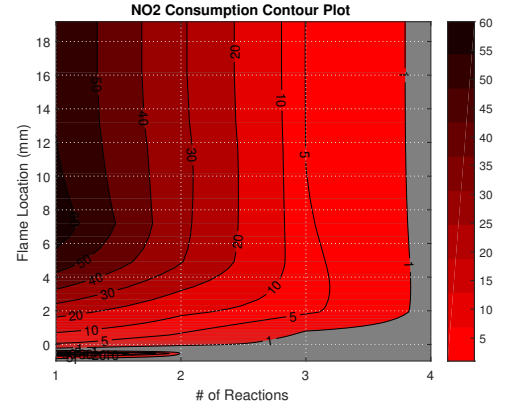


Figure 34:  $NO_2$  Consumption Contour Plot

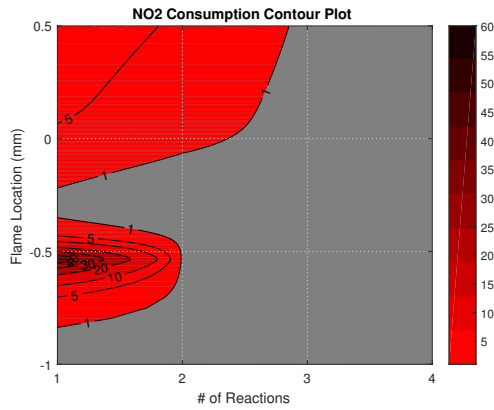


Figure 35:  $NO_2$  Consumption Reaction Layer Contour Plot

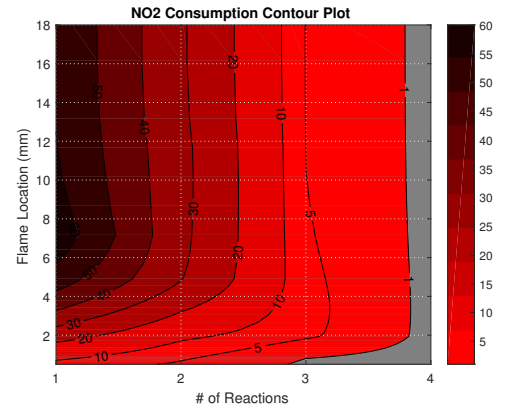


Figure 36:  $NO_2$  Consumption Post Flame Contour Plot

When analyzing the reaction tables for the consumption of  $NO_2$ , it can be seen that the same reactions are used throughout the flame with the exception of an addition reaction 186r for the reaction layer and also reaction 187r in the post flame region. All three benchmarks require the same number of reactions in each region because these reactions represent more than a 5% contribution, therefore 90% accuracy cannot be achieved without taking all the reactions for the 99% benchmark into account.

Table 11:  $NO_2$  Consumption Pre-Heat Region

Consumption Pre-Heat Region				
#	90%	95%	99%	Reaction
1	188f	188f	188f	$NO_2 + O \leftrightarrow NO + O_2$
2	189f	189f	189f	$NO_2 + H \leftrightarrow NO + OH$

Table 12:  $NO_2$  Consumption Reaction Layer

Consumption Reaction Layer				
#	90%	95%	99%	Reaction
1	188f	188f	188f	$NO_2 + O \leftrightarrow NO + O_2$
2	189f	189f	189f	$NO_2 + H \leftrightarrow NO + OH$
3	186r	186r	186r	$HO_2 + NO \leftrightarrow NO_2 + OH$

Table 13:  $NO_2$  Consumption Post Flame Region

Consumption Post Flame Region				
#	90%	95%	99%	Reaction
1	189f	189f	189f	$NO_2 + H \leftrightarrow NO + OH$
2	186r	186r	186r	$HO_2 + NO \leftrightarrow NO_2 + OH$
3	188f	188f	188f	$NO_2 + O \leftrightarrow NO + O_2$
4	187r	187r	187r	$NO + O + M \leftrightarrow NO_2 + M$

Figures 37 and 38 illustrate the trends of these reactions. Reaction 188f is the main contributing reaction in the reaction layer, but decays in contribution to be around the same importance as the other 3 reactions needed.

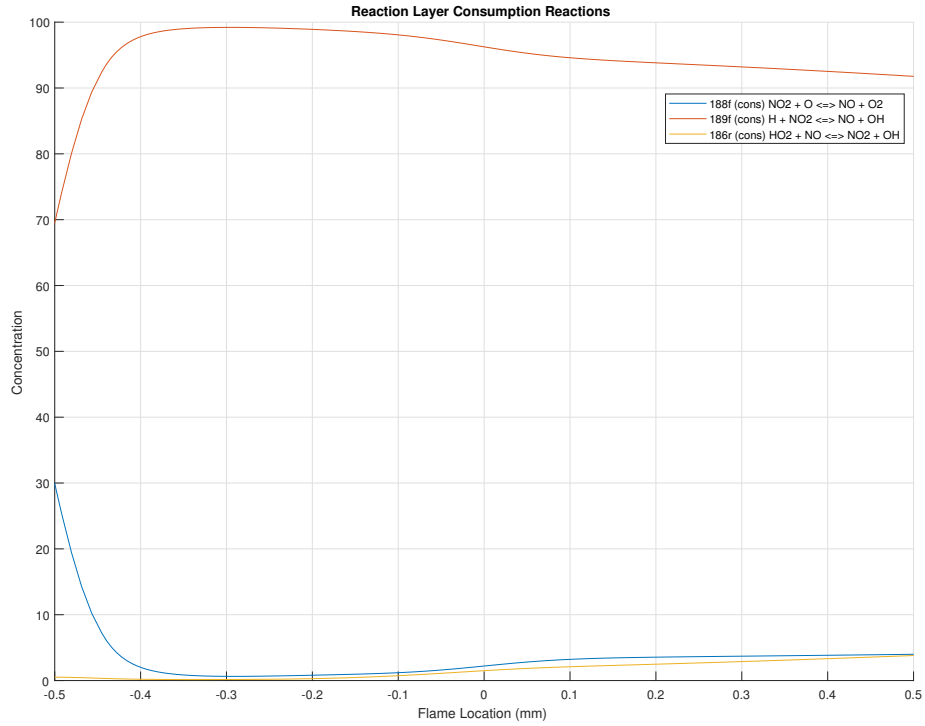


Figure 37:  $NO_2$  Reaction Layer Consumption Reactions

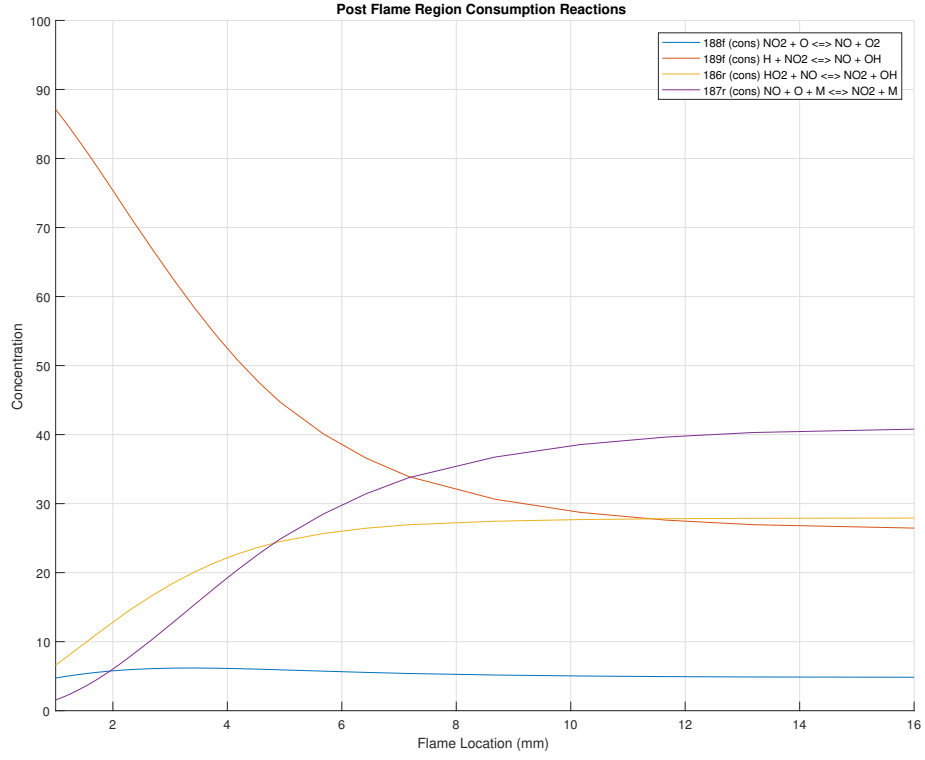


Figure 38:  $NO_2$  Post Flame Consumption Reactions

Just as was seen in the consumption reactions, the production result revolve around three to four reactions that describe  $NO$  throughout the flame. Reactions 186f, 187f, 189r are relevant in the entirety of the flame while the 99% benchmark requires the edition of only 188r in the post-flame.

Table 14:  $NO_2$  Consumption Pre-Heat Region

Consumption Pre-Heat Region				
#	90%	95%	99%	Reaction
1	-	-	-	—

Table 15:  $NO_2$  Production Reaction Layer

Production Reaction Layer				
#	90%	95%	99%	Reaction
1	186f	186f	186f	$HO_2 + NO \leftrightarrow NO_2 + OH$
2	187f	187f	187f	$NO + O + M \leftrightarrow NO_2 + M$
3	-	-	189r	$NO_2 + H \leftrightarrow NO + OH$



Table 16:  $NO_2$  Production Post Flame

Production Post Flame				
#	90%	95%	99%	Reaction
1	187f	187f	187f	$NO + O + M \leftrightarrow NO_2 + M$
2	186f	186f	186f	$HO_2 + NO \leftrightarrow NO_2 + OH$
3	189r	189r	189r	$NO_2 + H \leftrightarrow NO + OH$
4	-	-	188r	$NO_2 + O \leftrightarrow NO + O_2$

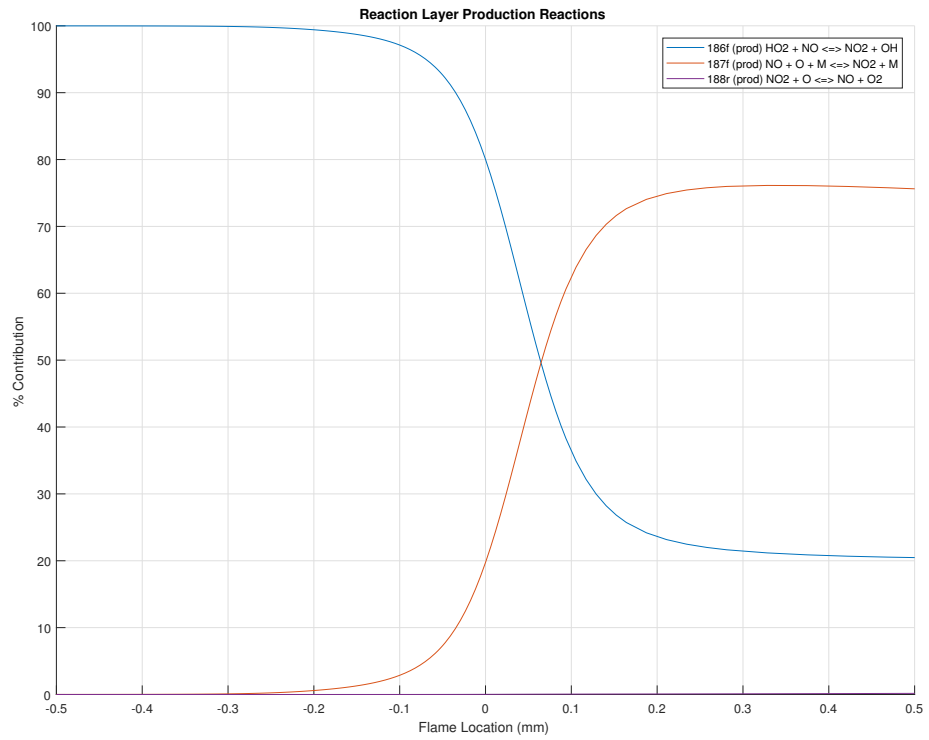


Figure 39:  $NO_2$  Reaction Layer Production Reactions

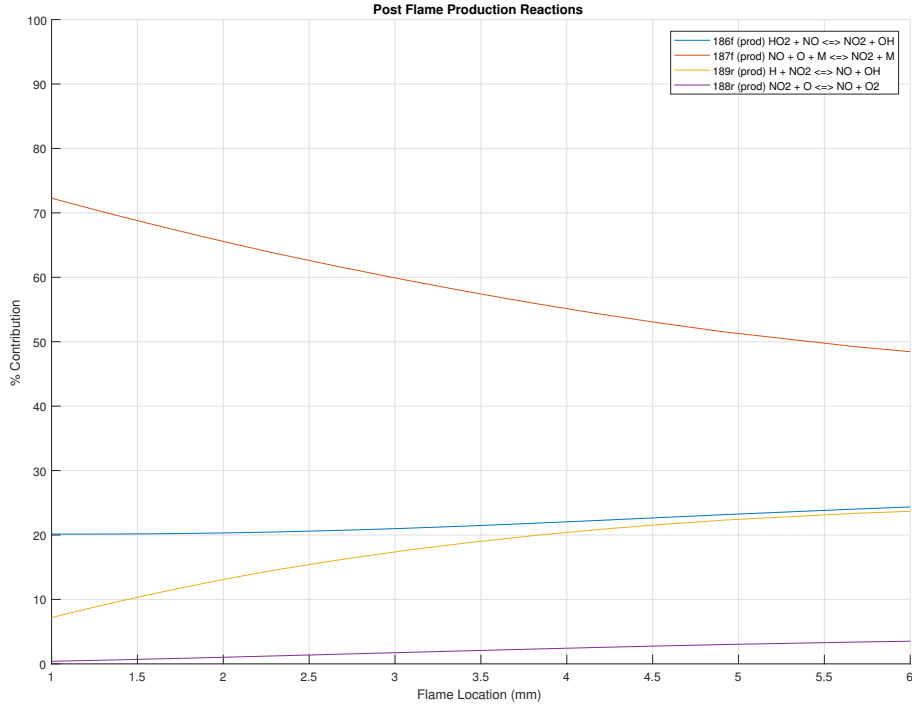


Figure 40:  $NO_2$  Post Flame Production Reactions

Similar to  $NO$ , the reactions for  $NO_2$  can be compiled into a single list of reactions to describe the species' production and consumption. It can be seen that four reactions must be kept in order to achieve the desired accuracy for every benchmark. The reactions kept for  $NO_2$  are also kept for the  $NO$  mechanism as well, therefore their concentrations are directly related.

Table 17:  $NO_2$  Required Reactions

$NO_2$ Required Reactions				
#	90%	95%	99%	Reaction
1	186	186	186	$HO_2 + NO \leftrightarrow NO_2 + OH$
2	187	187	187	$NO + O + M \leftrightarrow NO_2 + M$
3	188	188	188	$NO_2 + O \leftrightarrow NO + O_2$
4	189	189	189	$NO_2 + H \leftrightarrow NO + OH$

In the same way  $NO$  was checked for the steady state approximation,  $NO_2$  must also be evaluated. Figure 40 graphically shows that the steady state approximation can be applied to  $NO_2$ . The percent error is maintained at approximately zero for the entire in the flame.

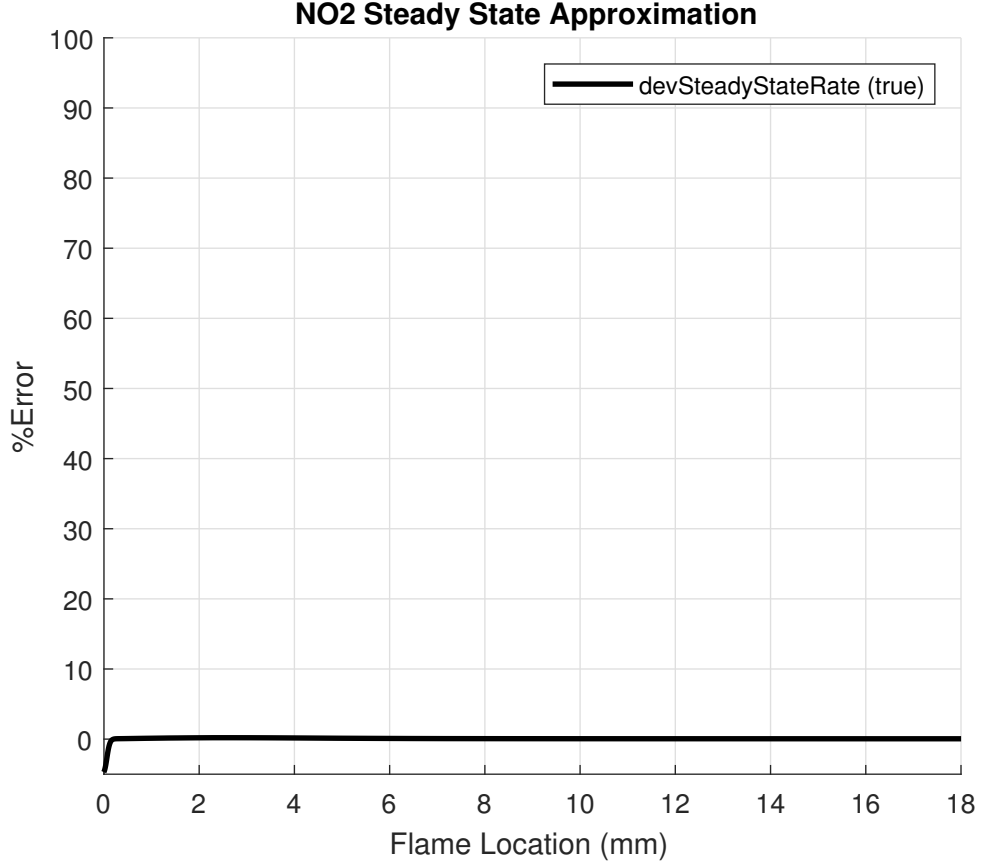


Figure 41:  $NO_2$  Steady State Approximation

Similar to the steps taken for  $CN$  in the methods section, the steady state relation can be formed for  $NO_2$ . The relationship developed from setting the reaction rates and concentrations of the consumption and production reactions equal to each other is

$$[NO_2] = \frac{[NO] \left( k_{187f}[O] + k_{186f}[HO_2] + k_{189r}[OH] + k_{188r}[O_2] \right)}{\left( k_{189f}[H] + k_{186r}[OH] + k_{188f}[O] + k_{188r}[O_2] \right)}$$

Now, it can clearly be seen that  $NO_2$  is only dependent on one nitrogen based species,  $NO$ .  $NO_2$  is also dependent on the concentrations of  $O$ ,  $HO_2$ ,  $OH$ ,  $O_2$ , and  $H$  radicals as well as temperature which can be written as

$$[NO_2] = f([NO], [O], [HO_2], [OH], [O_2], [H], T)$$

which, again, is much simpler for computer simulation rather than calculating the advection and diffusion terms for every point in the flame.

### 4.3 Overview

#### Steady State

Once the analysis conducted for  $NO$  and  $NO_2$  has applied to every nitrogen based species involved in the production and consumption of  $NO_x$  has been analyzed, a list of steady state and non steady state species can be generated.

Table 18: Steady State Species Approximation

Steady State Species Approximation	
Not Steady State	Steady State
$NO$	$NO_2$
$HCN$	$CN$
$HNCO$	$H_2CN$
$HOCN$	$HCNO$
$N_2$	$HNO$
$N_2O$	$N$
$NH_3$	$NCO$
—	$NH$
—	$NH_2$

Since the species have now been split into steady state and non steady state, the steady state assumption can now be applied to the appropriate species. Recalling that the steady state assumption allows for the production of a species to be set equal to its consumption and the process conducted in the methods section for  $CN$ , the following relations can be made.

$$[CN] = \left[ \frac{[HCN] \left( k_{219r}[OH] + k_{233f}[O] + k_{221f}[H] \right) + [NCO] \left( k_{220r}[O] + k_{218r}[H] \right) + [N_2] \left( k_{239f}[C] \right)}{\left( k_{220f}[O_2] + k_{221f}[H_2] + k_{219f}[OH] + k_{218f}[OH] + k_{217f}[O] + k_{233f}[OH] \right)} \right]$$

$$[NO_2] = \frac{[NO] \left( k_{187f}[O] + k_{186f}[HO_2] + k_{189r}[OH] + k_{188r}[O_2] \right)}{\left( k_{189f}[H] + k_{186r}[OH] + k_{188f}[O] + k_{188r}[O_2] \right)} \quad (36)$$

$$[H_2CN] = \frac{[N] \left( k_{275f} \right) + [HCN] \left( k_{237f}[H] \right) + [NO] \left( k_{256f}[CH_3] \right)}{\left( k_{237r}[M] + k_{238f}[N] \right)} \quad (37)$$

$$[HCNO] = \left[ \frac{[NO] \left( k_{251f}[CH_2] + k_{274f}[HCCO] + k_{254f}[CH_2(s)] \right) + [HCN] \left( k_{271r}[OH] \right) + [HNCO] \left( k_{270r}[H] \right) + [NH_2] \left( k_{272r}[CO] \right)}{\left( (k_{220f} + k_{271f} + k_{272f} + k_{251r})[H] \right)} \right] \quad (38)$$

$$[HNO] = \left[ \frac{[NO] \left( k_{212f}[H][M] + k_{215r}[H_2O] + k_{216r}[HO_2] + k_{214r}[H_2] + k_{213r}[OH] \right) + [NH] \left( k_{193f}[OH] + k_{197f}[H_2O] + k_{280f}[CO_2] + k_{194f}[O_2] \right) + [NH_2] \left( k_{201f}[O] \right)}{\left( k_{215f}[OH] + k_{280r}[CO] + k_{216f}[O_2] + k_{213f}[O] + (k_{214f} + k_{192r})[H] + k_{197r}[H_2] + k_{212r}[M] \right)} \right] \quad (39)$$

$$[N] = \left[ \frac{[NH] \left( k_{193f}[OH] + k_{191f}[H] \right) + [N_2] \left( k_{240f}[CH] + k_{178r}[O] \right) + [CN] \left( k_{217f}[O] \right) + [NO] \left( k_{248f}[CH] + k_{180r}[H] + k_{179r}[O] \right)}{\left( k_{179f}[O_2] + (k_{275f} + k_{276f})[CH_3] + k_{180f}[OH] + k_{283f}[CO_2] + k_{193r}[H_2O] \right)} \right] \quad (40)$$

$$[NCO] = \frac{\begin{aligned} &[HNC O] \left( k_{267f}[OH] + k_{264f}[O] + k_{266f}[H] \right) \\ &+ [CN] \left( k_{220f}[O_2] + k_{218f}[OH] \right) + [NH] \left( k_{223r}[CO] \right) \\ &+ [HCN] \left( k_{231f}[O] \right) + [N_2O] \left( k_{228r}[CO] \right) \\ &+ [N_2] \left( k_{229r}[CO_2] \right) + [N] \left( k_{227r}[CO][M] \right) \\ &+ [NO] \left( k_{224r}[H][CO] + k_{247f}[CH] \right) \end{aligned}}{\begin{aligned} &\left( k_{266r}[H_2] + k_{282f}[NO_2] + (k_{224f} + k_{264r})[OH] \right. \\ &+ (k_{229f} + k_{228f})[NO] + (k_{222f} + k_{220r})[O] + k_{267r}[H_2O] \\ &+ (k_{223f} + k_{231r})[H] + k_{264r}[OH] + k_{227f}[M] + k_{226f}[O_2] \left. \right) \end{aligned}} \quad (41)$$

$$[NH] = \frac{\begin{aligned} &[NH_2] \left( k_{203f}[OH] + k_{200f}[O] + k_{202f}[H] \right) \\ &+ [HNO] \left( k_{280r}[CO] + k_{197r}[H_2] + k_{192r}[H] \right) \\ &+ [NCO] \left( k_{223f}[H] \right) + [HCN] \left( k_{232f}[O] \right) \\ &+ [N_2O] \left( k_{199r}[H] \right) + [HNC O] \left( k_{262f}[O] \right) \\ &+ [NNH] \left( k_{208f}[O] \right) \\ &+ [N] \left( k_{193r}[H_2O] + k_{191r}[H_2] \right) + [N_2] \left( k_{198r}[OH] \right) \end{aligned}}{\begin{aligned} &\left( (k_{195f} + k_{194f})[O_2] + k_{269r}[CO][M] \right. \\ &+ (k_{192f} + k_{193f})[OH] + k_{191f}[H] + k_{197f}[H_2O] \\ &+ k_{190f}[O] + k_{280f}[CO_2] + k_{202r}[H_2] + k_{203r}[H_2O] \left. \right) \end{aligned}} \quad (42)$$

$$\frac{d[NH_3]}{dt} = \frac{[NH_2] \left( k_{277r}[H_2] + k_{279r}[OH] + k_{278r}[H_2O] \right)}{\left( k_{278f}[OH] + k_{279f}[O] + k_{277f}[H] \right)} \quad (43)$$

where all of the equations relate the concentration of the chosen species to the reaction rates and concentrations of other nitrogen based species and their associated radicals. Again, these equations are much simpler than the equations

that would be derived if the advection and diffusion terms were not considered to be negligible. Now that these equations have been found, the concentrations of the steady state species can be defined as functions of their related species concentrations and temperature because the reaction rates are a function of temperature.

$$[CN] = f\left([HCN], [NCO], [N_2], [OH], [O], [H], [C], [O_2], [H_2], T\right) \quad (44)$$

$$[NO_2] = f\left([NO], [O], [HO_2], [OH], [O_2], [H], T\right) \quad (45)$$

$$[H_2CN] = f\left([N], [HCN], [NO], [N], [H], [CH_3], T\right) \quad (46)$$

$$[HCNO] = f\left([NO], [HCN], [HNCO], [NH_2], [H], [CH_2], [HCCO], [CH_2(s)], [OH], [CO], T\right) \quad (47)$$

$$[HNO] = f\left([NO], [NH], [NH_2], [H], [HO_2], [H_2], [OH], [CO_2], [O_2], [O], [CO], T\right) \quad (48)$$

$$[N] = f\left([NH], [N_2], [CN], [NO], [OH], [H], [CH], [O], [O_2], [CH_3], [CO_2], [H_2O], T\right) \quad (49)$$

$$[NCO] = f\left([HCN], [HNCO], [CN], [NH], [N_2O], [N_2], [N], [NO_2], [NO], [O], [OH], [H], [O_2], [CO], [CH], [H_2], [H_2O], T\right) \quad (50)$$

$$[NH] = f\left([NH_2], [HNO], [NCO], [HCN], [NNH], [N_2O], [HNCO], [N], [N_2], [OH], [O], [H], [CO], [H_2], [H_2O], [O_2], [CO_2], T\right) \quad (51)$$

$$[NH_3] = f\left([NH_2], [H_2], [OH], [H_2O], [O], [H], T\right) \quad (52)$$

## Mechanism Reduction

After compiling all of the reactions deemed important for each benchmark, the mechanism can be reduced and simulated through Cantera to validate the reductions. Then, the percent deviation in concentration of the reduced

mechanisms from the original full GRI-Mech 3.0 mechanism were calculated using the following equation at every point in the flame.

$$PercentError = \frac{[Y_i]_{reducedmech} - [Y_i]_{fullmech}}{[Y_i]_{fullmech}} * 100 \quad (53)$$

The percent error was then graphed for each species where the percent deviation as a function of the flame location. In order for the reduction to be proven, the percent deviation cannot be greater than the set benchmark reduction. In other words, there should only be up to a 1% deviation for the 99% benchmark, 5% deviation for the 95% benchmark, and a 10% deviation for the 90% benchmark. Now, analyzing these graphs for the two main  $NO_x$  species, it is clear to see that the reduction process used is viable.

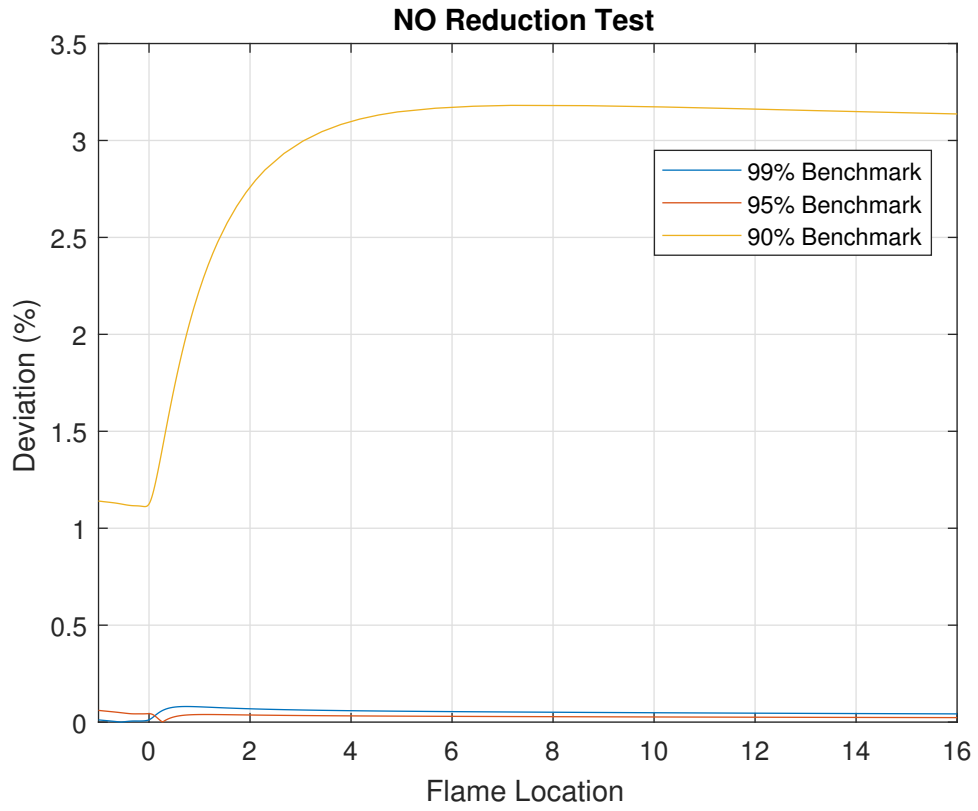


Figure 42:  $NO$  Mechanism Reduction Test



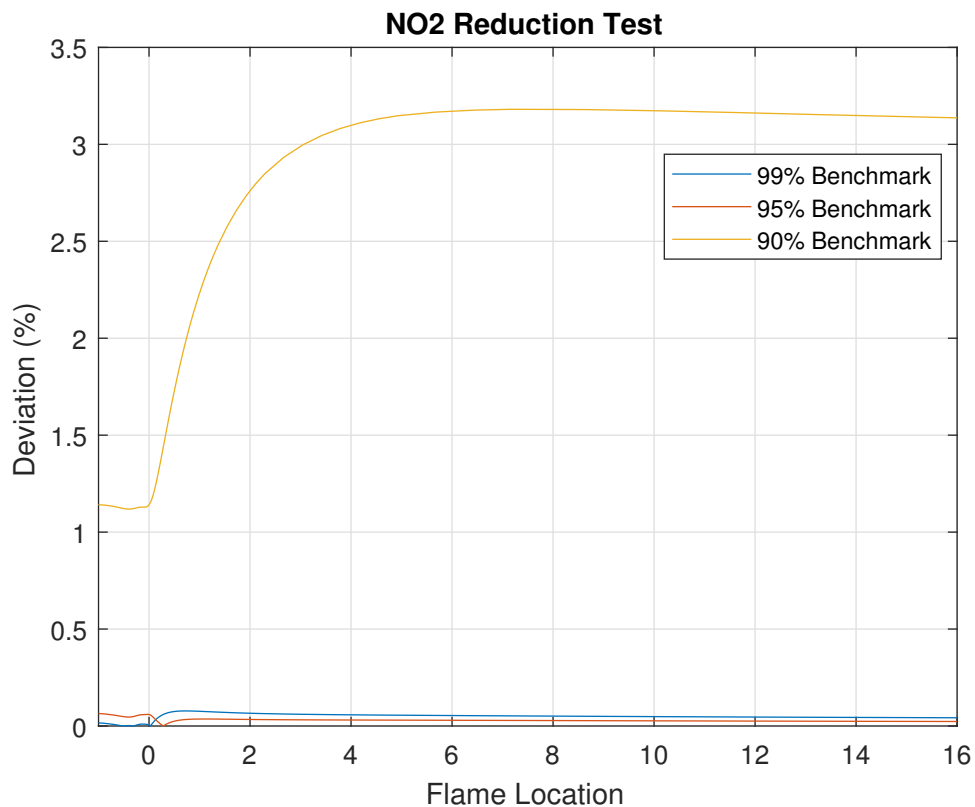


Figure 43:  $\text{NO}_2$  Mechanism Reduction Test

With the reductions proven, the efficiency of the reductions can be stated. In the original GRI-Mech 3.0 mechanism, there are 109 reactions that involve nitrogen based species. For each benchmark, the percent reduction of nitrogen based reactions were calculated. The total mechanism was reduced to 79, 84, and 92 reactions for the 90%, 95%, and 99% benchmark reduced mechanisms respectively which is a 28%, 23%, and 16% decrease in reactions.

## 5 Conclusion

In conclusion, through the principles of chemical kinetics in physical chemistry, discovered by Arrhenius and Bodenstein, the algorithm used in this skeletal reduction process has been proven viable for the considered  $NO_x$  mechanism. Considering the benchmarks of 90%, 95%, and 99% that result in the 28%, 23%, and 16% decrease respectively as well as the identified quasi-steady state species, the computing time of turbulent flames using these mechanism reductions will greatly decrease. The next step is determining the benefit of accuracy vs. computing time in which the reduced mechanism is tested in several turbulent flame conditions and plotting the results. Again, the algorithm developed in this paper can be set to any accuracy value and is not strictly for  $NO_x$  chemistry. The algorithm can be applied to any type of mechanism to quickly identify the most important species and reactions for the chosen case. Also, the reductions are a function of flame location, so if a portion of the flame is of most interest in a simulation, then the reduction can be applied at that location only. Future work can also include the investigation of the skeletal reduction of the  $NO_x$  mechanism along with the QSS assumption and how they change with heavier hydrocarbons or stoichiometric/rich flames.

# Appendix

## CN

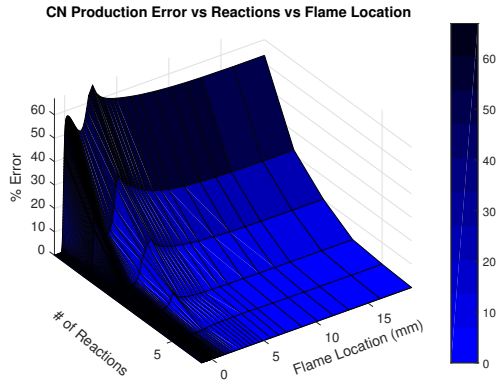


Figure 44: *CN* Production Surface Plot

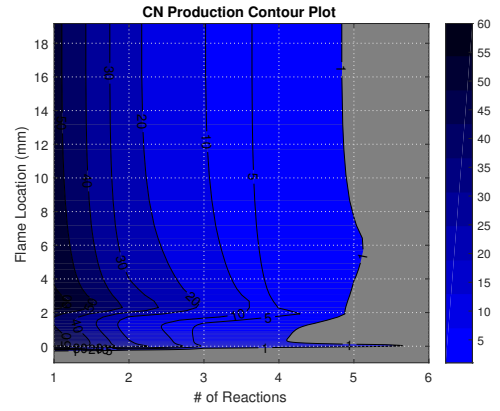


Figure 45: *CN* Production Contour Plot

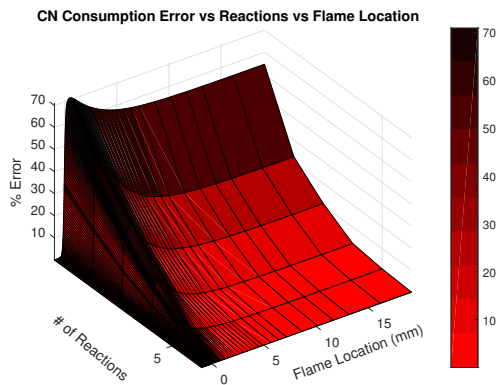


Figure 46: *CN* Consumption Surface Plot

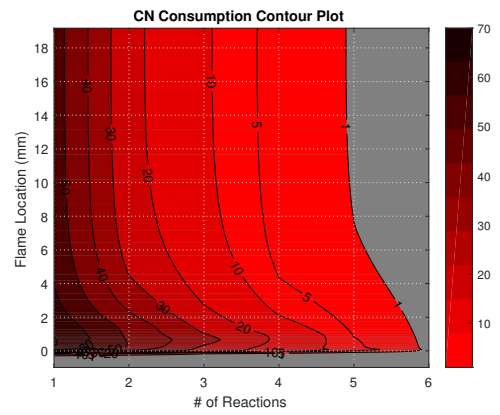


Figure 47: *CN* Consumption Contour Plot

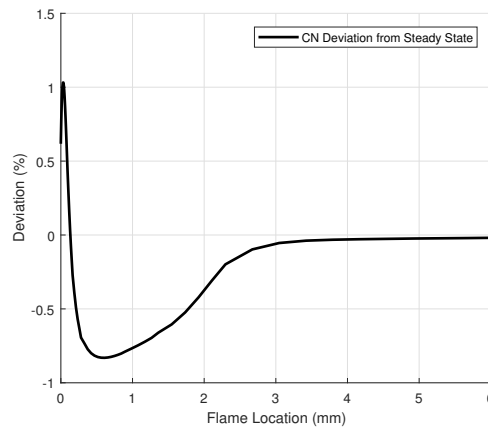


Figure 48: *CN* Steady State Approximation

## HCN

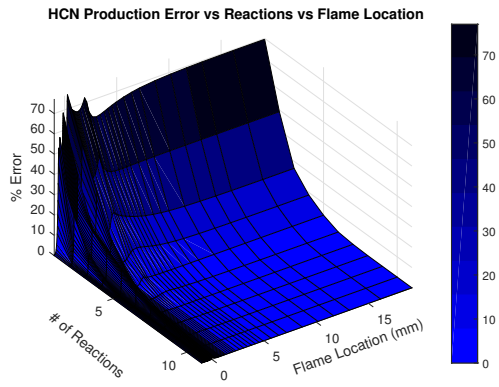


Figure 49: *HCN* Production Surface Plot

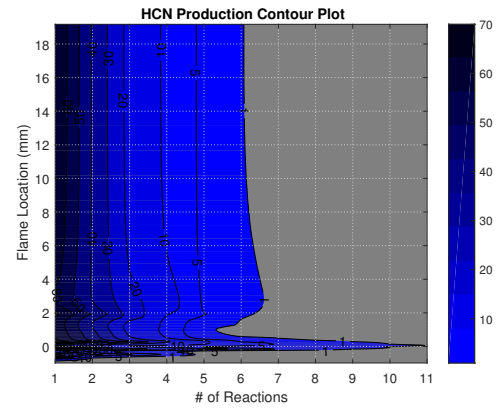


Figure 50: *HCN* Production Contour Plot

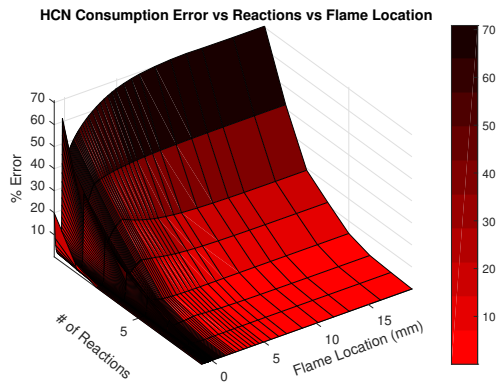


Figure 51: *HCN* Consumption Surface Plot

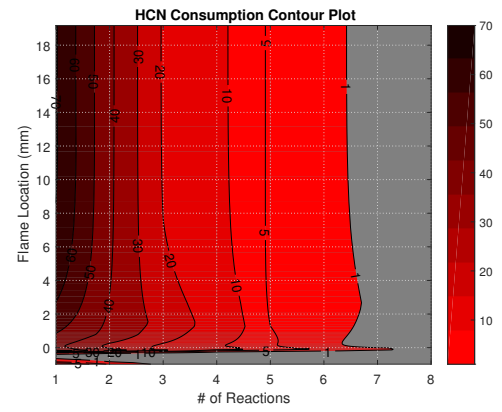


Figure 52: *HCN* Consumption Contour Plot

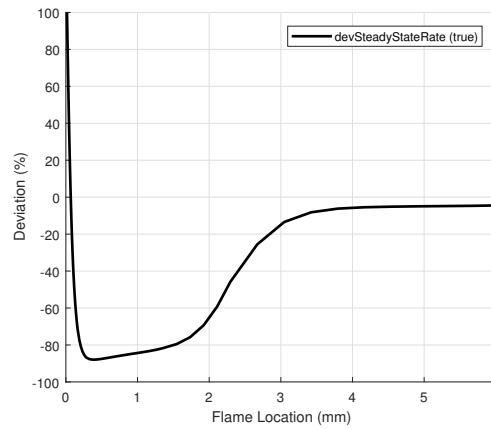


Figure 53: *HCN* Steady State Approximation

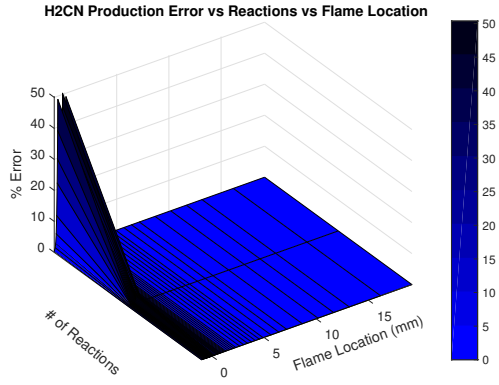
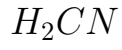


Figure 54:  $H_2CN$  Production Surface Plot

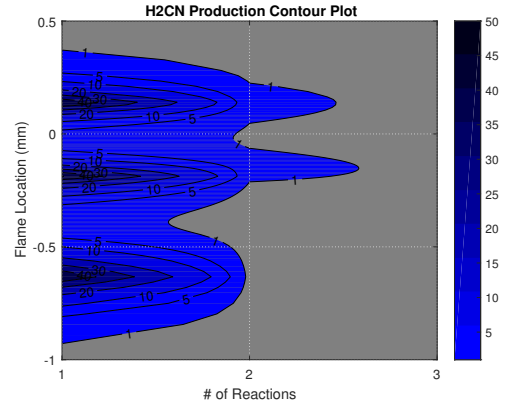


Figure 55:  $H_2CN$  Production Contour Plot

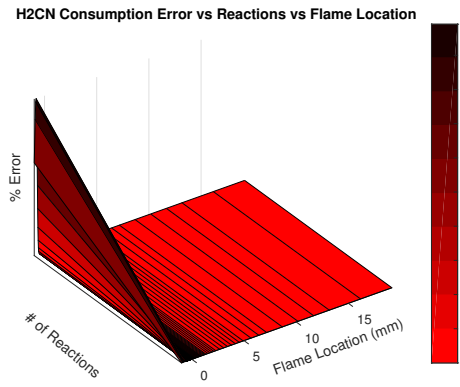


Figure 56:  $H_2CN$  Consumption Surface Plot

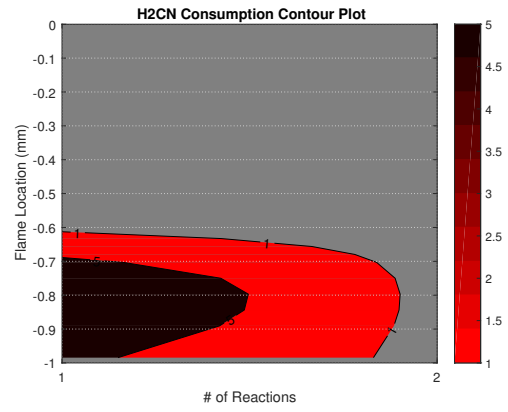


Figure 57:  $H_2CN$  Consumption Contour Plot

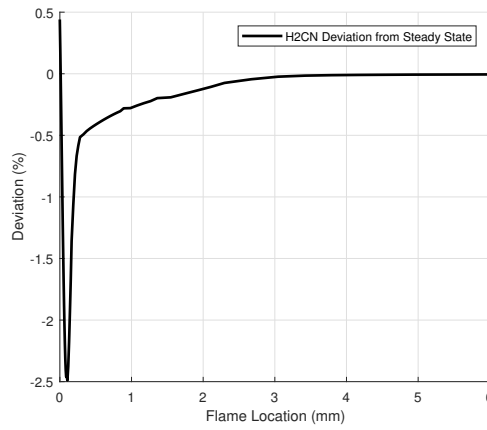


Figure 58:  $H_2CN$  Steady State Approximation

# $HCNO$

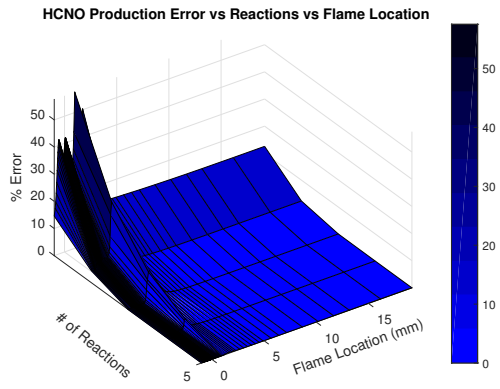


Figure 59:  $HCNO$  Production Surface Plot

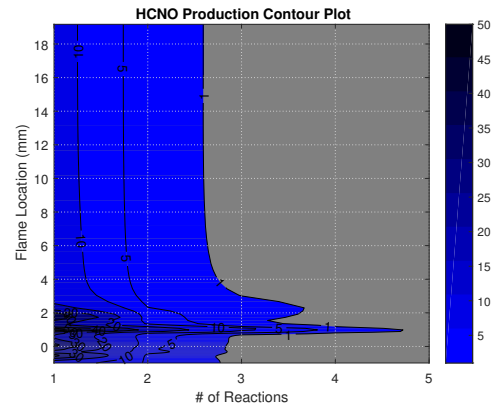


Figure 60:  $HCNO$  Production Contour Plot

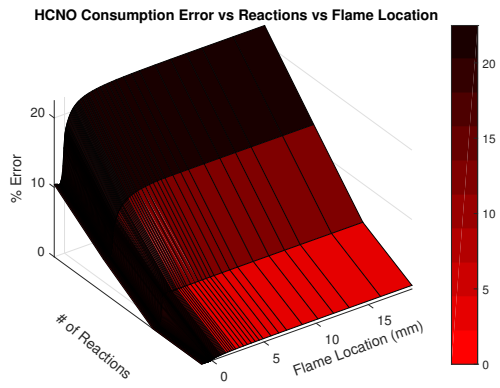


Figure 61:  $HCNO$  Consumption Surface Plot

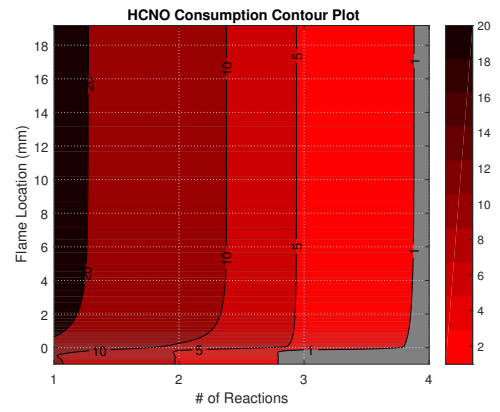


Figure 62:  $HCNO$  Consumption Contour Plot

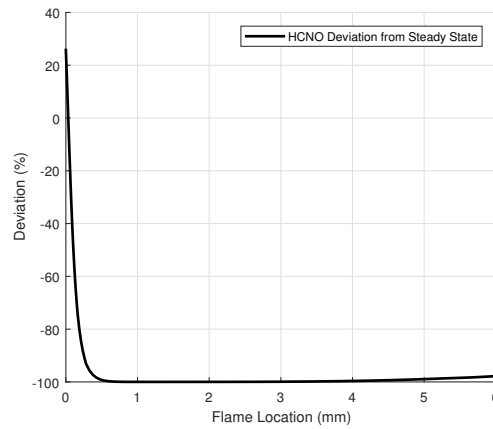


Figure 63:  $HCNO$  Steady State Approximation

*HNCO*

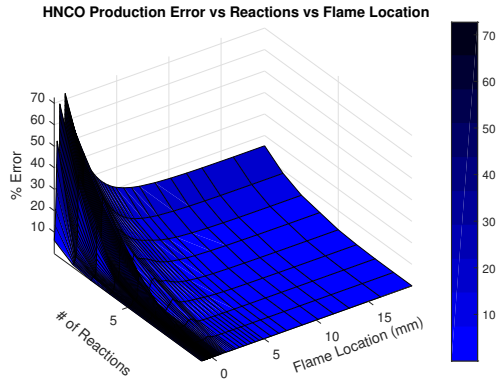


Figure 64: *HNCO* Production Surface Plot

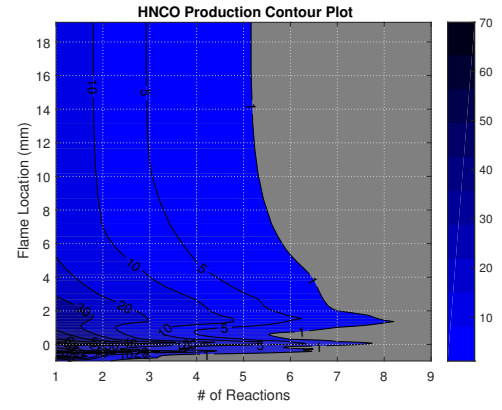


Figure 65: *HNCO* Production Contour Plot

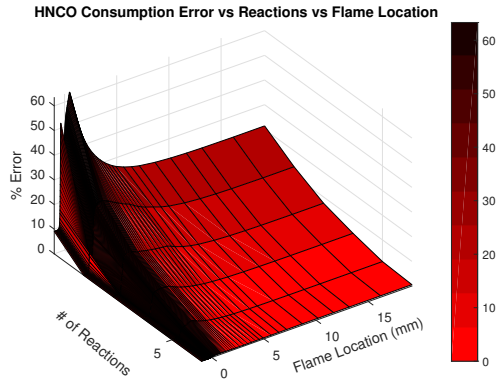


Figure 66: *HNCO* Consumption Surface Plot

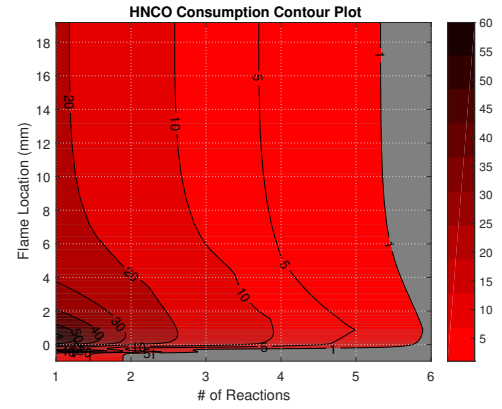


Figure 67: *HNCO* Consumption Contour Plot

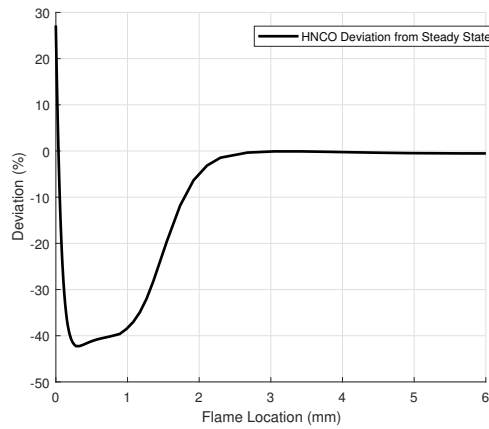


Figure 68: *HCNO* Steady State Approximation

# $HNO$

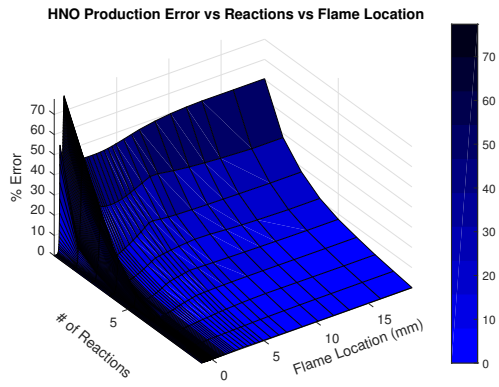


Figure 69:  $HNO$  Production Surface Plot

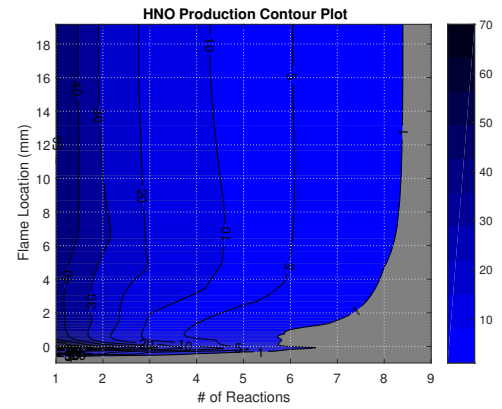


Figure 70:  $HNO$  Production Contour Plot

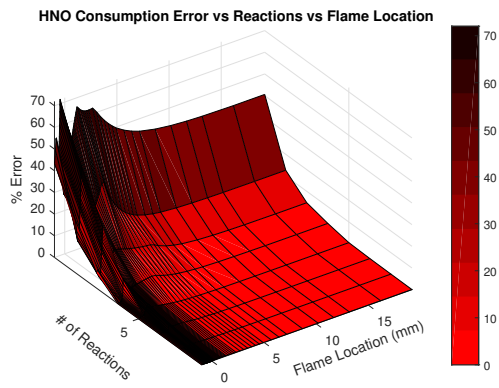


Figure 71:  $HNO$  Consumption Surface Plot

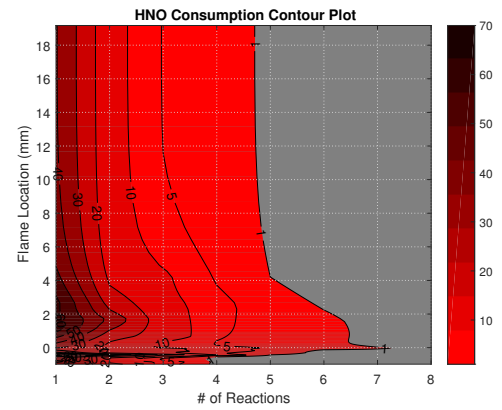


Figure 72:  $HNO$  Consumption Contour Plot

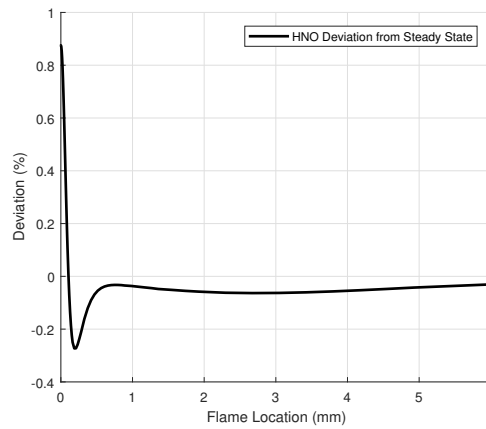


Figure 73:  $HNO$  Steady State Approximation



## *HOCN*

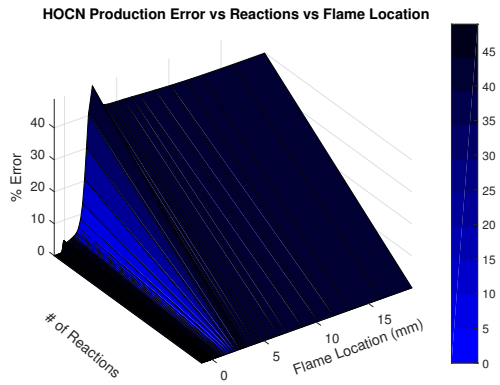


Figure 74: *HOCN* Production Surface Plot

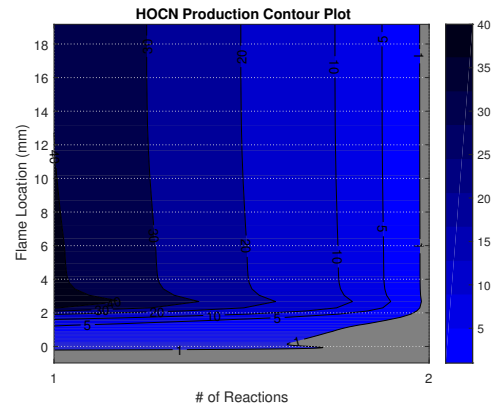


Figure 75: *HOCN* Production Contour Plot

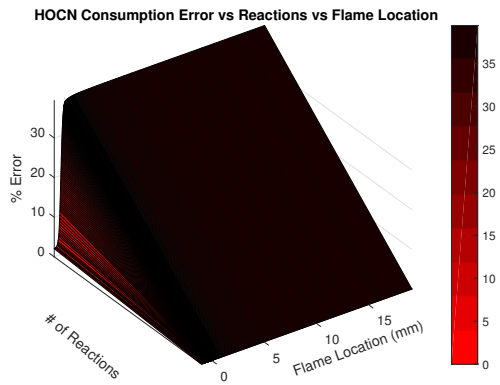


Figure 76: *HOCN* Consumption Surface Plot

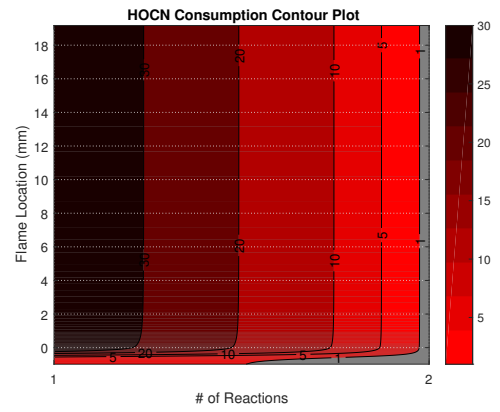


Figure 77: *HOCN* Consumption Contour Plot

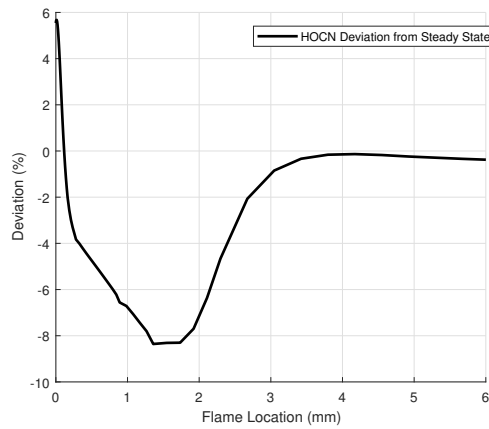


Figure 78: *HCNO* Steady State Approximation

$N$

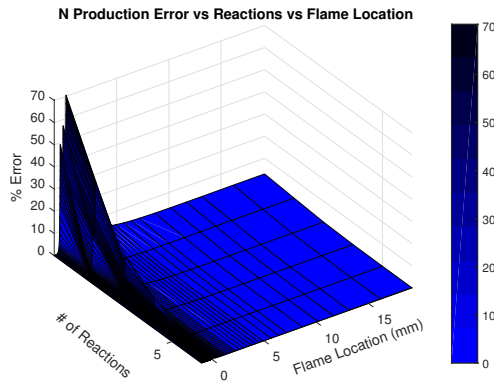


Figure 79:  $N$  Production Surface Plot

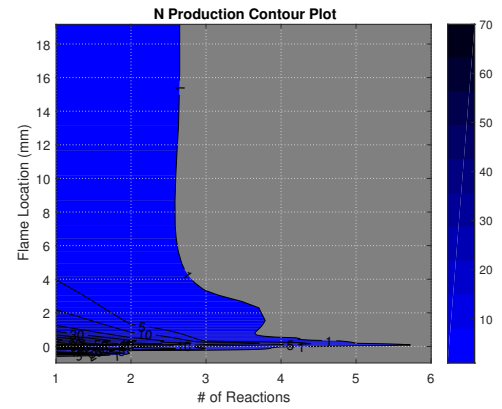


Figure 80:  $N$  Production Contour Plot

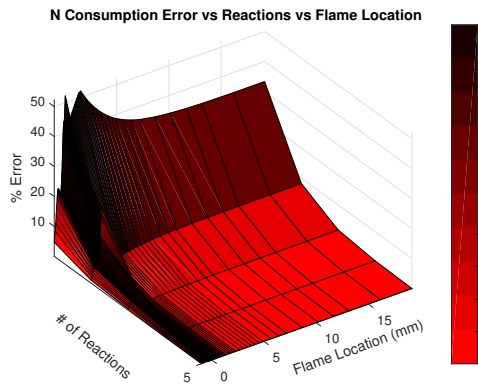


Figure 81:  $N$  Consumption Surface Plot

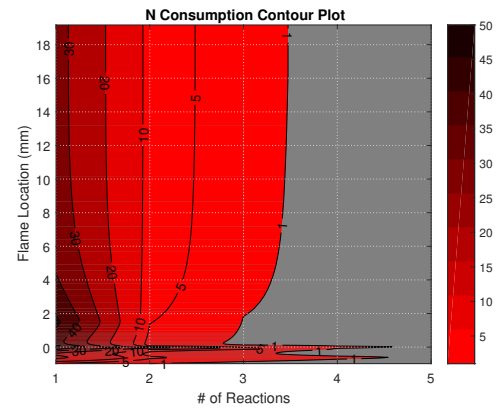


Figure 82:  $N$  Consumption Contour Plot

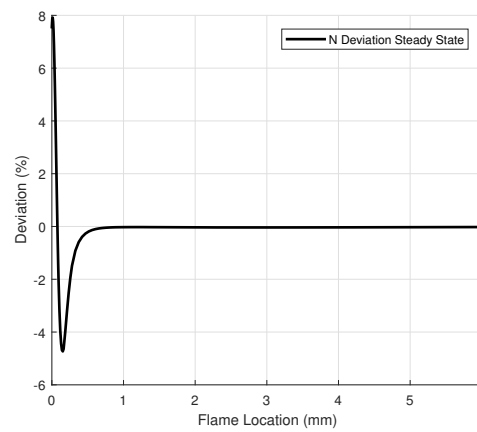


Figure 83:  $N$  Steady State Approximation

$N_2$

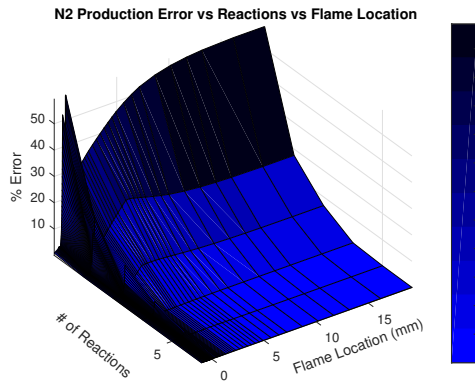


Figure 84:  $N_2$  Production Surface Plot

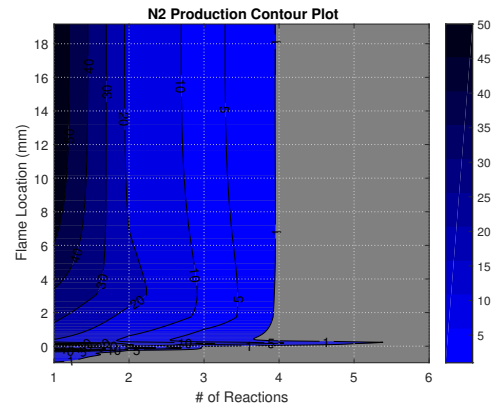


Figure 85:  $N_2$  Production Contour Plot

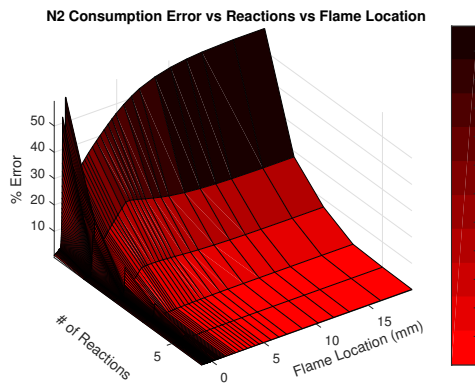


Figure 86:  $N_2$  Consumption Surface Plot

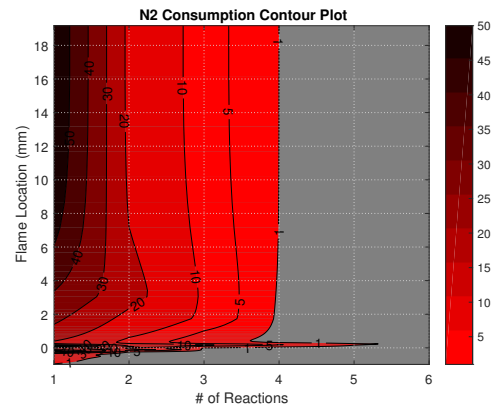


Figure 87:  $N_2$  Consumption Contour Plot

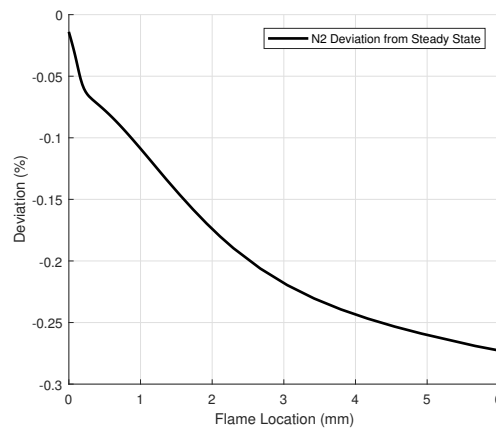


Figure 88:  $N_2$  Steady State Approximation

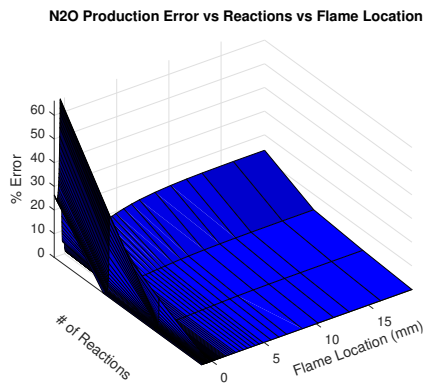


Figure 89:  $N_2O$  Production Surface Plot

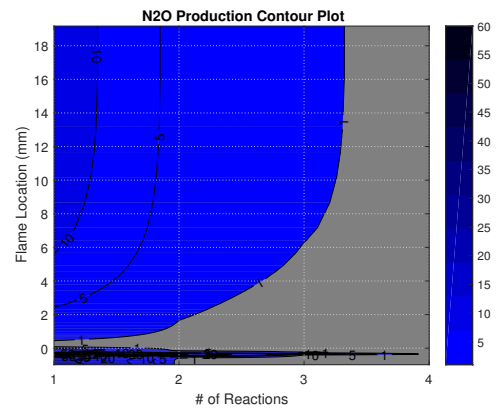


Figure 90:  $N_2O$  Production Contour Plot

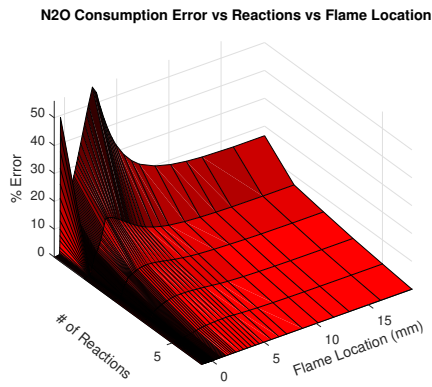


Figure 91:  $N_2O$  Consumption Surface Plot

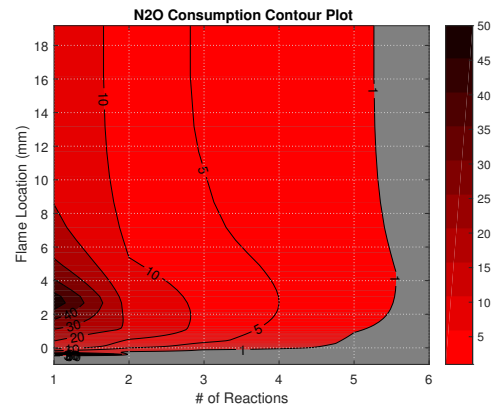


Figure 92:  $N_2O$  Consumption Contour Plot

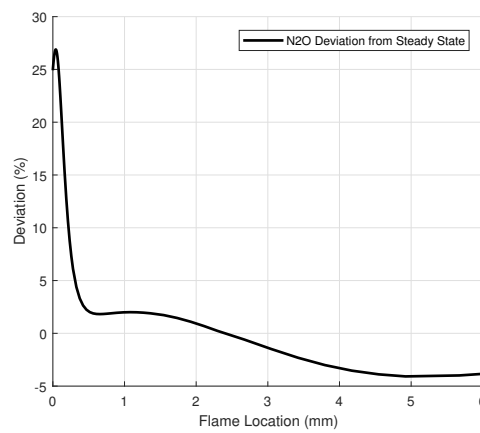


Figure 93:  $N_2O$  Steady State Approximation

*NCO*

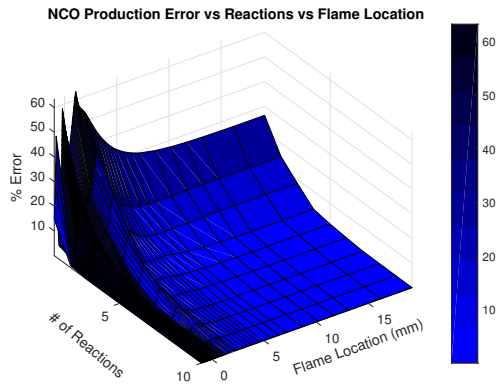


Figure 94: *NCO* Production Surface Plot

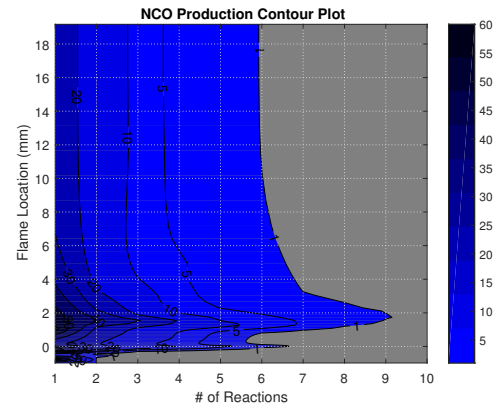


Figure 95: *NCO* Production Contour Plot

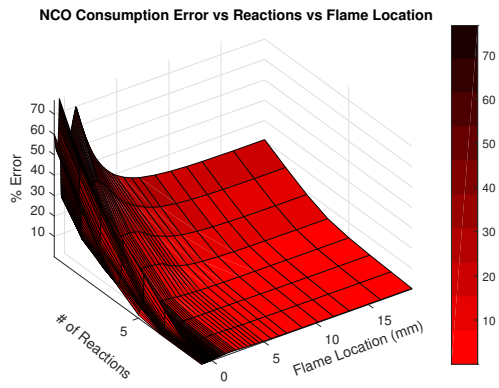


Figure 96: *NCO* Consumption Surface Plot

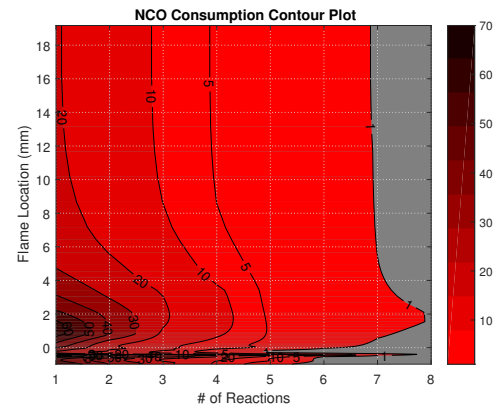


Figure 97: *NCO* Consumption Contour Plot

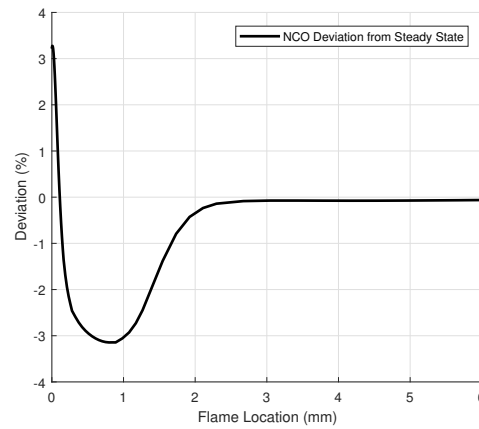


Figure 98: *NCO* Steady State Approximation

$NH$

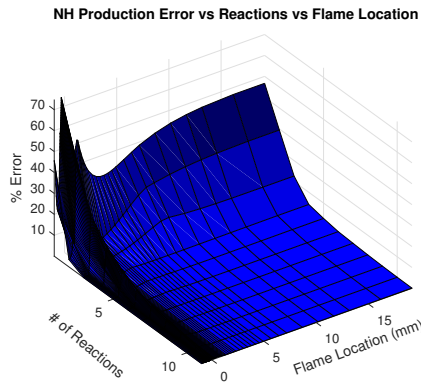


Figure 99:  $NH$  Production Surface Plot

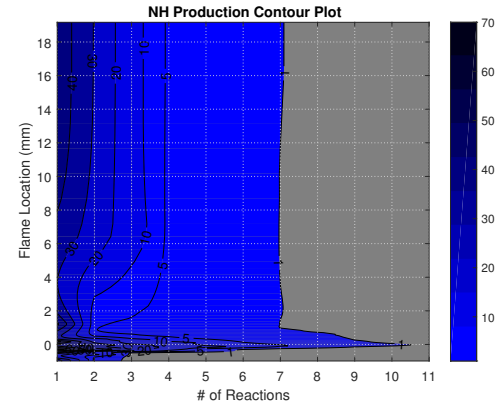


Figure 100:  $NH$  Production Contour Plot

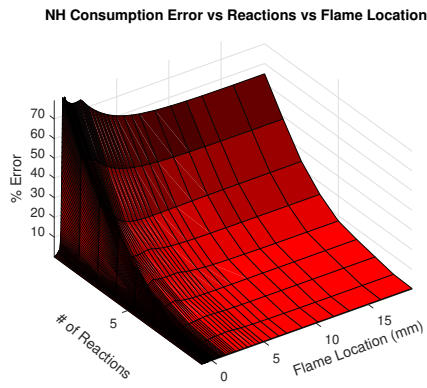


Figure 101:  $NH$  Consumption Surface Plot

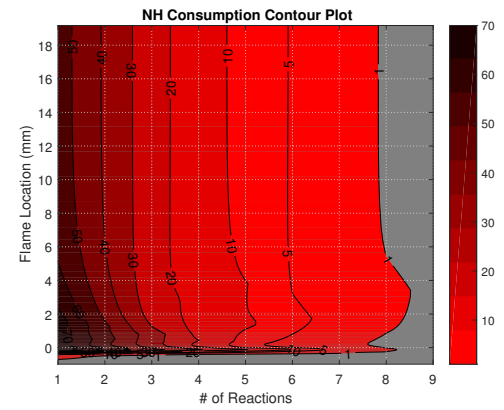


Figure 102:  $NH$  Consumption Contour Plot

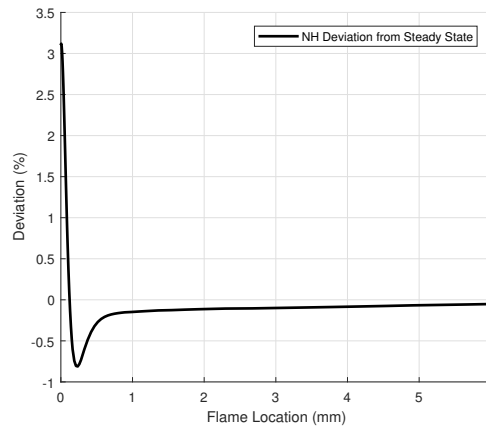


Figure 103:  $NH$  Steady State Approximation

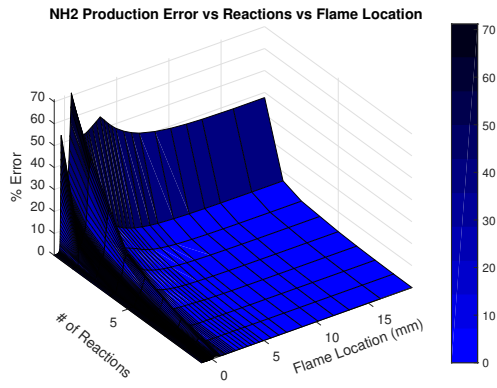


Figure 104:  $NH_2$  Production Surface Plot

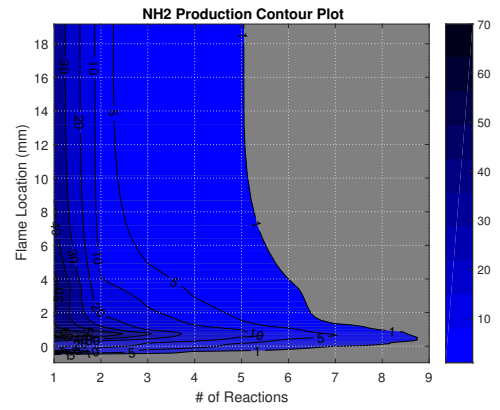


Figure 105:  $NH_2$  Production Contour Plot

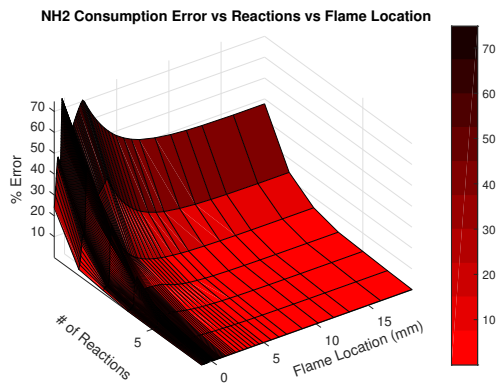


Figure 106:  $NH_2$  Consumption Surface Plot

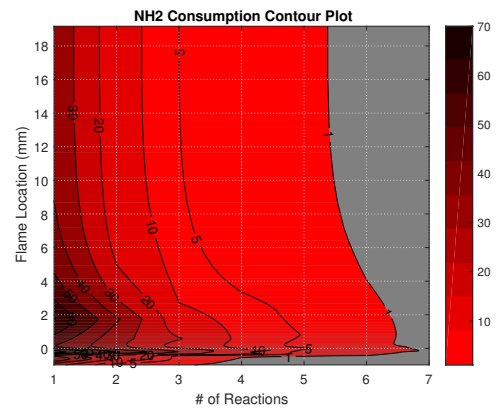


Figure 107:  $NH_2$  Consumption Contour Plot

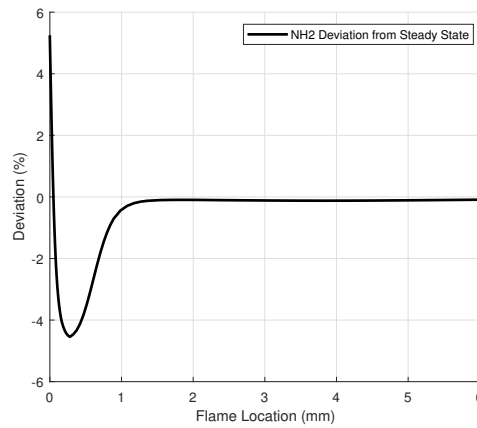


Figure 108:  $NH_2$  Steady State Approximation

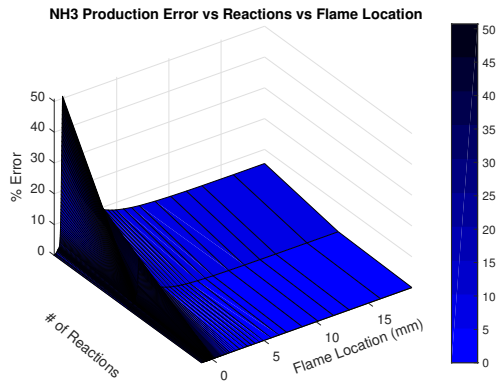


Figure 109:  $NH_3$  Production Surface Plot

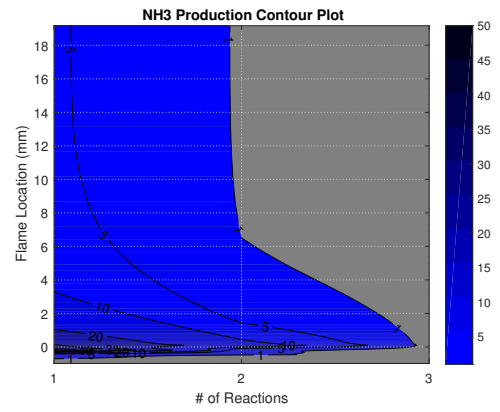


Figure 110:  $NH_3$  Production Contour Plot

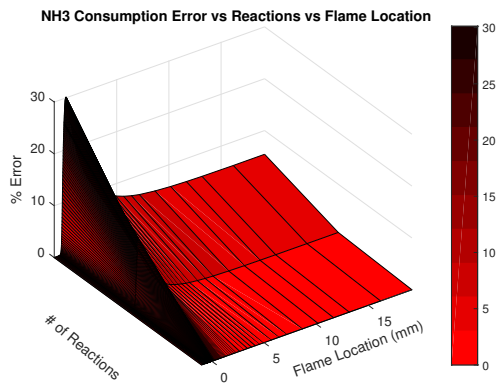


Figure 111:  $NH_3$  Consumption Surface Plot

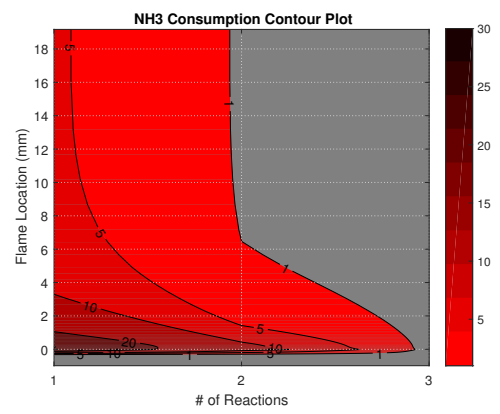


Figure 112:  $NH_3$  Consumption Contour Plot

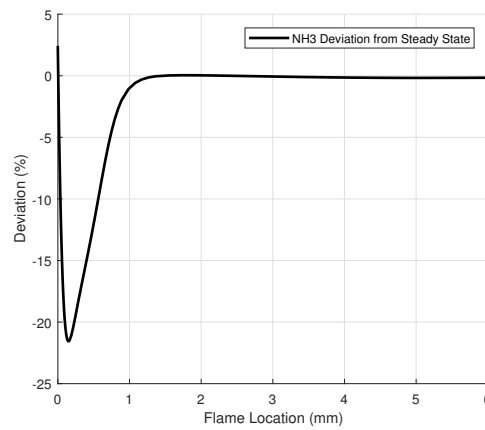


Figure 113:  $NH_3$  Steady State Approximation



## References

- [1] United States, Congress, Blaszcak, Robert, and Lyndon Cox. *Nitrogen Oxides (NO<sub>x</sub>): Why and How They Are Controlled.*, U.S. Environmental Protection Agency, Office of Air Quality Planning and Standards, Information Transfer and Program Integration Division, Clean Air Technology Center, 1999.
- [2] David G. Goodwin, Harry K. Moffat, and Raymond L. Speth. *Cantera: An object- oriented software toolkit for chemical kinetics, thermodynamics, and transport processes*. <http://www.cantera.org>, 2017. Version 2.3.0. doi:10.5281/zenodo.170284
- [3] Guldberg CM, Waage P. Studier i affiniteten. Forhandlinger: Videnskabs Selskabet i Christiana, 1864; 35
- [4] Harcourt, A.v., and W. Esson. *On The Laws Of Connexion Between The Conditions Of A Chemical Change And Its Amount*. Selected Readings in Chemical Kinetics, 1967, pp. 3–27., doi:10.1016/b978-0-08-012344-8.50004-0.
- [5] Hoff, J. H. van't, et al. *Studies in Chemical Dynamics*. F. Muller, 1896. pp. 122-142.
- [6] OSTWALD, Friedrich Wilhelm., and William White. TAYLOR. *Outlines of General Chemistry ... Translated ... by W.W. Taylor ... Third Edition*. London, 1912. pp. 286-302.
- [7] Arrhenius, S. *On the Influence of Carbonic Acid in the Air upon the Temperature of the Earth*. Publications of the Astronomical Society of the Pacific, vol. 9, 1897, p. 14., doi:10.1086/121158.
- [8] Chapman, David Leonard, and Leo Kingsley Underhill. *The Interaction of Chlorine and Hydrogen. The Influence of Mass*. J. Chem. Soc., Trans., vol. 103, 1913, pp. 496–508., doi:10.1039/ct9130300496.
- [9] M. Bodenstein, Eine Theorie der photochemischen Reaktionsgeschwindigkeiten, Z. Phys. Chem. (1913) 85, 390–421
- [10] Williams, F. A. *Combustion Theory the Fundamental Theory of Chemically Reacting Flow Systems*. Perseus Books, 1985.
- [11] Fenimore, C.p. *Formation of Nitric Oxide in Premixed Hydrocarbon Flames*. Symposium (International) on Combustion, vol. 13, no. 1, 1971, pp. 373–380., doi:10.1016/s0082-0784(71)80040-1.
- [12] Saito, Kozo. *Basic Combustion Phenomena*. Formation and Reduction of Nitrogen Oxides.
- [13] Frenklach, M., in *Combustion Chemistry* (W. C.Gardiner, Jr., Ed.), Springer-Verlag, New York, 1984, chap. 7.
- [14] Frenklach, M., Kailasanath, K., and Oran, E. S., Prog. Astronaut. Aeronaut. 105:365-376 (1986).

- [15] Wang, Hai, and Michael Frenklach. *Detailed Reduction of Reaction Mechanisms for Flame Modeling*. Combustion and Flame, vol. 87, no. 3-4, 1991, pp. 365–370., doi:10.1016/0010-2180(91)90120-z.
- [16] Frenklach, Michael, et al. *Optimization and Analysis of Large Chemical Kinetic Mechanisms Using the Solution Mapping Method*. Combustion of Methane. Progress in Energy and Combustion Science, vol. 18, no. 1, 1992, pp. 47–73., doi:10.1016/0360-1285(92)90032v.
- [17] T. Turanyi, *New J. Chem.* 14, (1990), pp. 795-803
- [18] A.S. Tomlin, M.J. Pilling, T. Turanyi, J.H Merkin, J. Brindley, *Combust. Flame* 91(2), (1992), pp. 107-130.
- [19] A.S. Tomlin, T. Turanyi, M.j. Pilling, *Comprehensive Chemical Kinetics*. Elsevier, Amsterdam, 1997, pp. 293-370.
- [20] Pepiotdesjardins, P, and H Pitsch. *An Efficient Error-Propagation-Based Reduction Method for Large Chemical Kinetic Mechanisms*. Combustion and Flame, vol. 154, no. 1-2, 2008, pp. 67–81., doi:10.1016/j.combustflame.2007.10.020.
- [21] Xin, Yuxuan, et al.  
The Directed Relation Graph Method for Mechanism Reduction in the Oxidative Coupling Catalysis Today, vol. 131, no. 1-4, 2008, pp. 483–488., doi:10.1016/j.cattod.2007.10.065.
- [22] Maaren, A. Van, et al. *Measurement of Flame Temperature and Adiabatic Burning Velocity of Methane/Air Mixtures*. Combustion Science and Technology, vol. 96, no. 4-6, 1994, pp. 327–344., doi:10.1080/00102209408935360.
- [23] “Tianfeng Lu.” Reduced Mechanisms, University of Connecticut, [www.engr.uconn.edu/~tlu/mechs/mechs.htm](http://www.engr.uconn.edu/~tlu/mechs/mechs.htm).

## Vita

1. Place of birth: Columbus, IN
2. Education/Degrees: BSME from the University of Kentucky
3. Professional positions held: N/a
4. Professional publications: N/a
5. Robert T. Hughes